

SUPPLEMENTARY INFORMATION

Supplementary Figure Legends

Supplementary Figure 1. Analysis of Gene Expression profiles from In Vitro cultured Primary Mammary Epithelial Cells.

A. Immunofluorescence staining of organoid cultures at the indicated time points for Ki67(magenta), Cleaved caspase-3 (green) and Dapi (blue), highlighting the oncogene induced proliferation (Ki67) and the caspase-3 dependent clearing of the organoids following oncogene withdrawal. Following oncogene inactivation organoids regress to a dormant population, as illustrated by the Ki67 staining of representative structures at 7 and 28 days following oncogene inactivation. Timepoints included in the staining: Never Induced, 2.5 Days ON Dox, 5 Days ON Dox, 12 Hours OFF Dox, 7 Days OFF Dox and 28 Days OFF Dox. Scale bar represents 50 μm

B. Quantitative RT-PCR for cMYC, NEU, and KRAS^{G12D} transgene expression in organoid cultures. RNA was collected from Never Induced Structure, Doxycycline Induced for 5 day structures and Regressed structures (5 Day Doxycycline induction followed by doxycycline withdrawal, regressed time point taken 7 days post-Doxycycline withdrawal.)

C. Ingenuity pathway analysis was used for pathway enrichment analysis of differentially expressed genes from the regressed condition compared to the Never Induced (control) state. Down Regulated networks are those enriched in the negatively regulated gene-sets and are represented on the right. Up-regulated networks were those enriched in the over-represented gene sets (IPA®, QIAGEN Redwood City, www.qiagen.com/ingenuity). The analysis showed that the regressed state most strongly up-regulated cellular lipid metabolism, while genes involved in cell cycle progression and DNA damage repair pathways were down-regulated

D. GO slim Pie Charts generated using PantherDB (<http://www.pantherdb.org/>) for differentially regulated genes in the regressed dataset when compared to the never induced (left). The most overrepresented gene ontology group was “Metabolic Processes” with an enrichment of genes involved in lipid, nucleobase and protein metabolism. The Metabolic Pathways are broken down into 5 main sub-categories and is represented by the number of genes found deregulated in each sub-category (Right).

Supplementary Figure 2. Increased de novo Fatty Acid Biosynthesis in Regressed Mammary Glands

A. Plots representing the observed alterations in gene expression profiles for genes involved in fatty acid biosynthesis for the 5 Day ON and Regressed Datasets in respect to the control condition Never Induced in the MYC/KRAS data set. Scale bar represents 500 μm

B. Immunohistological staining of PPAR γ in mammary glands isolated from Never Induced, Primary Tumor and Regressed MYC/NEU mice.

C. Fatty acid concentration levels in cells isolated from MYC/NEU organoids for Never Induced, 5 Day ON and Regressed (n=4 for each condition) as detected by GC-MS. Metabolite levels were normalized first with ribitol as internal standard, then with TML (total metabolite levels normalization).

Supplementary Figure 3. Oxidative stress is a unique hallmark of oncogene induced mammary gland re-modeling.

A. Plots representing the observed alterations in NOXA gene expression profiles for 5 Day ON and Regressed Datasets in respect to the control condition Never Induced in the MYC/KRAS data set.

B. Plots representing the observed alterations in Anti-oxidant gene expression profiles for 5 Day ON and Regressed Datasets in respect to the control condition Never Induced in the MYC/KRAS data set.

C. Representative images for the detection of ROS in MYC/NEU organoids for the Never Induced, 5 Day ON and Regressed timepoints. Mitotracker was used to detect total mitochondria, DHE is a super-oxide detection reagent, and DCFDA is a global indicator of oxidative stress. Scale bar represents 50 μm

D. Representative images for the detection of ROS in MYC/NEU organoids for the Never Induced, 5 Day ON and Regressed timepoints. Mitotracker was used to detect total mitochondria, MitoSox is a super-oxide detection reagent, and DCFDA is a global indicator of oxidative stress. Scale bar represents 50 μm

E. DCFDA was added to previously published FACS based protocols for separation of mammary epithelial subpopulations. The panels on the left show representative FACS separation of sub-populations using previously published combination of CD29/CD24/CD49f for control and NEU regressed mice. The 3 panels on the right are representative histograms the Mean Fluorescent Intensities (MFI) of DCFDA in mammary epithelial cells isolated from age-matched control and regressed animals for the CD29^{hi}/CD24^{hi}/CD49f^{med} (luminal progenitors) CD29^{hi}/CD24^{med}/CD49f^{med} (Myoepithelial) and CD29^{hi}/CD24^{med}/CD49f^{hi} (Stem) populations. These results were representative for n=3 control and n=3 NEU independent experiments.

Supplementary Figure 4. Comparison of Gene Expression between Experimental Data Sets and Published (GSE40877) Dataset of Parity Induced Gene Expression

A. Venn diagram representing overlapping differentially regulated genes for the comparison between the MYC/KRAS Regressed v. Never Induced and Parous v. Nulliparous CD24^{hi}/Sca1-

populations. The comparison demonstrates minimal overlap between these two processes, highlighting the unique nature of oncogene induced mammary gland remodeling.

B. Gene set enrichment analysis (GSEA) overlap of differential genes associated with the CD24^{hi}/Sca1⁻ Parous v. Nulliparous animals (GSE40877) with MGSigDB curated gene sets; gene sets and corresponding P-values are represented (<http://www.broadinstitute.org/gsea/msigdb/annotate.jsp>)

Supplementary Figure 5. Increased levels of FASN, Lipid Stores and Oxidative stress in Organoids following treatment with Lapatanib

A panel of stainings to confront the consequences of oncogene inactivation by doxycycline withdrawal to that achieved through pharmacological inhibition by Lapatanib. Columns from left to right, Never Induced, Regressed, Never Induced/ Lapatanib treated, Regressed/Lapatanib treated. Stainings are indicated in the figure, and DAPI is in blue.

Supplementary Figure 6. Increased Levels of Oxidative DNA Damage in Cells Surviving Oncogene Inactivation

A. Immunofluorescence staining of mammary glands isolated from MYC/NEU regressed mice. In order to determine the baseline level of double strand breaks in regressed mammary glands they were stained for Lamin B1 and γ H2AX. Mammary glands isolated from mice subjected to total body 6 Gy irradiation were used as a control. Nuclei are counter-stained with DAPI. Scale bar represents 50 μ m

B. Immunohistochemical staining of age-matched control, MYC/KRAS and MYC/NEU regressed mammary glands taken 8-10 weeks post-regression for adduct 8-hydroxydeGuaninine(8-OHdG), a common adduct formed as a result of oxidative DNA damage. Images of representative of n=10 stainings for each condition. The scale bar represents 50 μ m

C. Schematic of modified comet assay (Left). Combination of Comet and modified Comet assay including formamidopyrimidine glycosylase (FPG) for measuring DNA damage and DNA adduct formation. Comet assay consists of embedding of organoid derived cells into an agarose layer, followed by cell lysis and in the case of FPG treatment, incubation with FPG. Followed by an alkali incubation and electrophoresis of samples. Fluorescence imaging was performed on a Leica LMD7000. Quantification of percent DNA in tail in FPG treated and non treated DNA isolated from regressed and age-matched control mammary glands; MYC/KRAS FPG v. Control FPG $P=0.0002$ MYC/NEU FPG v. Control FPG $P=0.0033$ (Right). Data are represented as mean \pm SEM of percentage DNA in found in the tail Comet for $n=3$ biological replicates per condition, $n=100$ comets scored using Image J PlugIn OpenComet (1). Significance was calculated using two tailed t -tests.

D. Western Blot analysis of Ogg1 levels in age-matched control, regressed mammary glands and regressed mammary glands isolated from mice that had been administered 40 mM NAC in the drinking water. α -Tubulin was used as a loading control (Left). Graphical Representation of the average of two technical replicates of the Ogg1 western represented on the left MYC/KRAS v. control $P=0.0201$, MYC/NEU v. control $P=0.0451$. Significance was calculated using an unpaired two-tailed t -test.

Error Bars denote mean \pm SEM * $p < 0.05$, ** $p < 0.01$, *** $p < 0.001$, **** $p < 0.0001$

Supplementary Figure 7. Confirmation of serial reseeded as a method to generate *in vitro* relapses, and functional controls for the treatment of *in vivo* cohorts.

A. Immunofluorescence staining for FASN and Nile Red detection of lipid droplets in serially reseeded cultures, following the fourth reseeded. From left: Never Induced (4th reseeded),

Regressed (4th reseeded), Never Induced+NAC (4th reseeded), Regressed+NAC (4th reseeded). Nuclei are stained with DAPI (blue). Scale bar represents 50 μ m

B. De novo somatic mutations are present in *in vitro* relapses. Left panel: Verification of the acquisition of a mutation in the rtTA region that drives re-expression of the oncogenes. Right panel: Immunohistochemical staining of MYC/KRAS spontaneous relapses and tumors which arose in Rag1^{-/-} mice following transplantation of *in vitro* cultured spontaneous relapses for human-cMYC. Scale bar represents 50 μ m.

C. Efficiency of N-acetylcysteine to scavenge reactive oxygen over one week period. Water was changed to fresh water containing 40 mM NAC on day 0 and animals (regressed and age-matched controls) were sacrificed for analysis of DCFDA at FACS on Days 1, 3, and 7. DCFDA readings are represented as fold change in MFI over the age-matched controls.

D. Treatment controls for both mifepristone and NAC treated animals. Upper panels represent vaginal smears collected on the day of L4 mammary gland surgery. Lower panel: BrdU immunohistochemistry on animals, which were administered BrdU in the drinking water for 48 hours (period spanning metestrus to diestrus). Panels include mifepristone implanted, age-matched control, and MYC/KRAS regressed mice. Scale bar represents 50 μ m.

Supplementary Figure 8. Overlapping Reactome Pathways and Reporter Metabolites found in neo-adjuvant human to mouse dataset comparisons

Venn diagram representing the comparison of over-represented Reactome pathways and reporter metabolites for genes that are differentially regulated following Neoadjuvant treatment in comparison to the pre-treatment biopsy. Two human datasets, a 7 patient cohort for which RNA-seq was performed on both pre- and post-therapy samples; human RNA-seq (yellow) and a previously published dataset (GSE32072) of pre- and post- neoadjuvant therapy samples (blue)

were analyzed along with the corresponding mouse; MYC/NEU and MYC/KRAS OFF versus 5Day_ON organoid datasets(red). The stromal gene signature was subtracted from all 4 datasets to allow for direct comparison. Human samples were not stratified for either breast cancer subtype or treatment regimen. Reactome pathways found in the overlaps for key lipid metabolic and signaling pathways and key reporter metabolites are listed for the 3-way intersection and the individual overlapping comparisons.

Supplementary Figure 9. Aberrant Lipid Metabolism Found in Cells Which Survive Neo-Adjuvant Therapies

A. Immunohistochemical staining for FASN of contralateral breast (control), triple negative, luminal and Her2 Neo-Adjuvant treated samples.

B. Immunohistochemical staining for 8OHdG of healthy breast (control), triple negative, luminal and Her2 Neo-Adjuvant treated samples. Quantification of percentage of nuclei staining positive was done in ImageJ and plotted in Prism. P-value <0.0001 for the comparison of percentage of 8-OHdG positivity to total nuclei between healthy breast and neo-adjuvant treated samples calculated using unpaired student t-test in Prism.

C. Immunohistochemical staining for Phospho-Histone H3 (ser10) of healthy breast (control), triple negative, luminal and Her2 Neo-Adjuvant treated samples. Quantification of percentage of nuclei staining positive was done in ImageJ and plotted in Prism. A non-significant P-value of 0.057 was calculated for the comparison of PH3 staining between healthy breast and neoadjuvant treated samples using unpaired student t-test in Prism.

D. Relapse Free Survival Curves for Breast Cancer Cases utilized in this study. Total Cases n=30, Triple Negative n= 9, Luminal n=10, Her2 n=11 cases.

*p < 0.05, **p < 0.01, ***p < 0.001, ****p<0.000

Supplementary Table 1. Metabolic pathways significantly de-regulated in the 5 day on and regressed organoid cultures. Metabolic pathways found to be significantly de-regulated for the comparison 5 day on v. Never Induced and Regressed v. Never Induced in the MYC/KRAS and MYC/NEU datasets.

Supplementary Table 2. Significantly de-regulated reporter metabolites following oncogene inactivation. Reporter metabolites found to be significantly de-regulated for the comparison Regressed v. Never Induced in the MYC/KRAS and MYC/NEU datasets.

Supplementary Table 3. Histopathological characterization and treatment regimes of RNA-SEQ samples. A comprehensive listing of the histopathological features, therapy regimes and survival statistics for the paired pre- and post-neoadjuvant treatment RNA-SEQ samples.

Supplementary Table 4. Significantly enriched Reactome Pathways following neoadjuvant therapy. Reactome pathways found to be enriched in the comparison post- versus pre-treatment in the 4 datasets: Human RNA-SEQ, Human GSE32072, and MYC/NEU and MYC/KRAS datasets depleted of their stromal signatures.

Supplementary Table 5. Significantly enriched reporter metabolites following neoadjuvant therapy. Reporter Metabolites found to be significantly de-regulated for the comparison post-versus pre-treatment in the 4 datasets: Human RNA-SEQ, Human GSE32072, and MYC/NEU and MYC/KRAS datasets depleted of their stromal signatures.

Supplementary Table 6. Histopathological characterization and treatment regimes of pre- and post-neoadjuvant treated tissue samples. A comprehensive listing of the histopathological features and therapy regimes for the paired pre- and post-neoadjuvant treatment human tissue samples.

Materials and Methods

Animals

NAC treatment of mice was administered in drinking water supplemented with 40 mg N-acetylcysteine (Sigma A7250) and changed weekly. Mifepristone slow release tablets were inserted subcutaneously at the base of the neck two weeks post-oncogene inactivation. As previously published, BrdU (Sigma B5002) was supplied in drinking water for 48 hours at a final concentration of 1 mg/mL(2). Inguinal mammary fat pad clearance was performed on 21- day old Rag1^{-/-} mice, which were subsequently used in transplantation experiments.

Human Breast Tissue Samples

The European Institute of Oncology (IEO) Division of Biostatistics selected from its institutional database 29 consecutive breast cancer (BC) patients fulfilling the following criteria: i) histologically proven invasive BC treated by neoadjuvant therapy; ii) any age (pre- or postmenopausal status allowed); iii) any intrinsic subtype (Luminal A/B-like, Her-2 positive, Triple Negative subtypes allowed); iv) failure in achieving a histologically documented pathologic complete response (no evidence of invasive tumor in the breast and axillary lymph nodes); v) availability of tissue from the diagnostic core biopsy and surgically excised post-therapy quadrantectomy/mastectomy. All the patients prospectively entered the IEO BC database and were discussed at the weekly multidisciplinary meeting. Data on patients' medical history, concurrent diseases, surgery, pathological evaluation, radiotherapy, neoadjuvant systemic treatments, and clinico-pathological results of pre- and post-neoadjuvant treatment staging procedures were retrieved. Neoadjuvant treatments were delivered in accordance with the best clinical practice guidelines: Briefly, Luminal A/B-like, Triple Negative and Her-2 positive BC patients received aromatase inhibitors, anthracyclines +/- Taxanes, other CHT combinations

containing anthracyclines +/- infusional therapy and Trastuzumab containing regimens, respectively. All the biopsies were fixed in 4% buffered formalin for less than 24 hours immediately after the core biopsy procedure. All the surgical samples were fresh sampled in accordance to the criteria issued by Provenzano et al. (2015) and fixed in 4% buffered formalin for less than 24 hours. All the biopsies and surgical samples were routinely processed and embedded in paraffin. Detailed information regarding tumor type and grade, ER/PgR and Her-2 *status*, and Ki-67 labeling index were available in all the cases. ER/PgR and HER2 immunoreactivity was assessed in line with the clinical practice procedures applicable at diagnosis. Her-2 immunoreactivity was assessed using the monoclonal antibody CB11 (Novocastra, 1:800) from 1995 till 2005, and the HercepTest (Dako) thereafter. Cases classified as Her-2 2+ by immunohistochemistry were tested by FISH analysis with Vysis probes, in accordance with the ASCO/CAP guidelines (Wolff, 2013). Ki-67 labeling index was assessed by the Mib-1 monoclonal antibody (Dako, 1:200), by counting at least 500 invasive tumor cells, independent of their staining intensity and without focusing on hot-spots (Polley, 2013). Tumors were classified as Luminal A-like (ER and PgR positive, absence of Her-2 overexpression and Ki-67 <20%), Luminal B-like (ER positive, Her-2 negative and at least one of Ki-67 \geq 20% and PgR <20%), Luminal B-like/Her-2 positive (ER and Her-2 positive, any PgR and Ki-67), Her-2 positive (Her-2 3+ and/or amplified by FISH, ER/PgR negative) and Triple Negative (ER, PgR and Her-2 negative) in accordance with St. Gallen recommendations (Coates, 2013). All the patients included gave an informed consent for using their clinico-pathological data and samples for research purposes at the time of admission to the hospital, and the study was approved by the IEO Review Board. Human breast samples for IHC analysis: The patients were not selected for a clinical trial specifically. All patients come from clinical practice, prospectively entered the IEO

BC database and gave an informed consent for using their clinico-pathological data and samples for research purposes at the time of admission to the hospital. The proceedings were approved by the IEO Review Board.

Human Breast Samples for RNA-SEQ

Neoadjuvant treated patients were selected from the "Genomstudy" of the University Women's Clinic Heidelberg (2009-2016). This study includes primary breast cancer cases that were newly diagnosed at the University women's clinic of Heidelberg and had given their informed consent for participating in this study. This study was approved by the Ethical Committee of the Medical Faculty in Heidelberg. All cases were female and Caucasian. Data on patient's concurrent diseases, surgery, pathological evaluation, radiotherapy, neoadjuvant systemic treatments, and clinico-pathological results of pre- and post-neoadjuvant treatment and follow-up data were retrieved.

Fresh core needle biopsies and fresh tumor tissue were examined by a pathologist, snap-frozen in liquid nitrogen and stored at -80°C within 15 min after sampling.

Total RNA as well as DNA and protein were extracted by applying the QIAGEN All Prep Kit. All eluates were stored at -80°C until usage.

Neoadjuvant treated patient samples for RNA-seq: The study entitled „Ermittlung neuer Zielproteine für kombinatorische Therapien bei Brustkrebs-Patientinnen sowie die Entwicklung prognostischer und prädiktiver Markerprofile“ with the study number S-039-2008 was approved by the Ethical Committee of the Medical Faculty in Heidelberg

Tissue culture and Reagents

Primary mammary cells were cultured according to previously published conditions(3). Briefly, primary mammary epithelial cells were isolated from 8 week old virgin female mice, through

mammary gland excision and digestion with collagenase, following seeding onto collagen plates (BD Biosciences) for selection of the epithelial population. Cells were trypsinized and seeded into a Type I Collagen (Cultrex® 3D Culture Matrix Rat Collagen I, Trevigen 3447-020-01) Matrigel (Cultrex® 3D Basement Membrane Matrix, Reduced Growth Factor, Trevigen 3445-005-01) 1:4 mixture (at a density of 10,000 cells per gel). Cultures were maintained in MEGM (MEGM™ Bullet kit, Lonza CC-3151 & CC-4136) at 37°C in 5% CO₂. Where appropriate, MEGM was supplemented with 20 µM N-acetylcysteine (Sigma A7250), 1 µg/mL Doxycycline (Doxycycline hyclate, Sigma D9891), 6 µg /ml C75 (Sigma C5490), 100 µM Etomoxir ((+)-Etomoxir sodium salt hydrate, Sigma E1095) and 500nM Lapatinib (Santa Cruz Biotechnologies sc-353658).

Immunofluorescence of gel embedded structures

Cells were seeded as described above and plated on Lab-tek chambers. After treatment, gels were fixed with 4% PFA for 10 minutes, following three washes with PBS. Cells were then blocked with 10% goat serum for 2 hours and IF was performed for Cleaved Caspase3 (Cell Signaling Technologies 96615), Ki67 (Dako M7249) E-cadherin (Invitrogen 131900, dilution 1:200), alpha-6 Integrin (Millipore MAB1378, dilution 1:80), FASN (Abcam ab128856, dilution 1:300) and ZO-1 (Life technologies 61-7300, dilution 1:500) according to standard protocol. Nuclei were counter stained with DAPI (Thermofischer 62248 1mg/ml, dilution 1:1000) in PBS for 10 minutes prior to mounting with Vectashield Anti-fade mounting medium (Vector Labs, H-1000), followed by imaging on a Leica SP5 Resonant Scanner and 63X water lens using the LAS AF imaging software.

Orthotopic recurrence

Orthotopic tumor recurrence assays were performed via injection of 50,000 cells into the inguinal mammary fat pad of cleared Rag1^{-/-} mice. The cells were obtained through isolation of *in vitro* relapses, which were expanded *in vitro*. Animals were monitored for tumor formation once weekly. Once the tumors reached 1 cm the experimental and control animals were sacrificed, and the tumors were fixed in formalin prior to embedding. The cMYC levels were detected by immunohistochemistry.

Tumor Regression and treatment

To evaluate the efficacy of the treatment protocols on delaying tumor recurrence, 8-10 week old adult mice were fed the doxycycline-enriched diet. Tumor onset was monitored once weekly until appearance of the primary tumor, at which time mice were monitored twice weekly. The mice were taken off the doxycycline-enriched diet when the total tumor burden reached 2 cm³. Mice which were used for FACS/ARP/IHC/Western analyses were allowed to regress for 8-10 weeks prior to sacrificing. For mice in treatment cohorts, regression was monitored and at two weeks post oncogene inactivation, mice were randomly separated into experimental cohorts. N-acetylcysteine treated mice were administered water supplemented with 40mm NAC, which was changed once weekly. Mifepristone treated mice had a slow release Mifepristone pill inserted subcutaneously at the base of the neck. Mice were monitored for recurrence weekly. Once spontaneous recurrence was detected, mice were monitored twice weekly, and were sacrificed when the tumor reached 1cm. Due to the nature of the treatment regime and the appearance of palpable mammary tumors, blinding was not feasible. Number of biological replicates for analysis (n=16 control, original n=10 for each experimental group) was set to allow for statistical testing.

Induction of Oncogenes

Oncogene expression is under the control of the doxycycline inducible MMTV-rtTA TetO system. In vitro expression was induced through the addition of doxycycline (Doxycycline hyclate, Sigma D9891) at a final concentration of 1 µg/mL to the culture media. The transgenic mice were induced through a diet containing doxycycline at 625 mg/kg (Mucedola)

Flow Cytometry Analysis

Mammary glands were dissected from regressed and age matched control mice. Following mechanical dissociation, the cells were prepared as described (4, 5). Cells were stained with rat anti-CD16/CD32 -CD45, -Ter119, -CD31, all from eBioscience (14-0161-86, 14-0451-82, 14-5921-82 and 14-0311-82 respectively) for 5 minutes. After washing in PBS/2% FBS, cells were stained with PE-Cy5 F(ab')₂ fragment of goat anti rat IgG (H+L) (Invitrogen A10691). After washing in PBS/2% FBS, cells were stained with anti-CD24-450 eFluor (eBioscience 48-0242-82), anti CD29-APC/Cy7 (Biolegend 102226) and anti-CD49f-PE (Millipore MAB1378) for 5 minutes at room temperature. Following washing with PBS/2% FBS, 100nm DCFDA was loaded for 20 minutes at 37°C and 5% CO₂. 7-AAD was added immediately prior to FACS. Samples were analyzed on a FACS ARIA flow cytometer (BD Biosciences). Data were analyzed using the FlowJo software (TreeStar). Number of biological replicates for analysis (n=9 control, n=3 parous, n=7 MYC/KRAS, n=3 MYC/NEU) was set to allow for statistical testing.

Live cell imaging

For live cell imaging of gel embedded structures, cells were seeded into matrigel and plated on chamber slides (Lab-Tek). Cells were pre-incubated with 5 µm MitoSox (MitoSOX™, ThermoFisher Scientific M36008) and Hoescht33342 (1µg/mL; Invitrogen H3570) for 2 hours at 37°C and 5% CO₂ followed by subsequent washing in warm PBS. Cells were loaded with 20 µm DCFDA (2',7'-Dichlorofluorescein diacetate, Sigma D6883-250MG) for 15 minutes prior to

imaging. For the purpose of ROS detection in cytoplasm and mitochondria, cells were pre-incubated with 5 μ M MitoSox or 1 μ M DHE (Dihydroethidium, ThermoFisher Scientific D1168) and 200 nM MitoTracker (MitoTracker® Deep Red FM, ThermoFisher Scientific M22426) for 1 hour at 37°C and 5% CO₂, with addition of 20 μ M DCFDA for 15 minutes prior to imaging. Images were obtained on a Leica SP5 Resonant Scanner equipped an environmental chamber which maintained the cells at 37°C and 5% CO₂ with a 63X water lens using the Leica LAS AF imaging software.

Nile Red Staining

Cells were stained according to previously published protocols(6). Briefly, gel imbedded structures were fixed in 4% PFA, then washed in PBS. Nile Red (Sigma N3013) was dissolved at 1 mg/mL in DMSO then diluted to a final concentration of 100ng/mL in 150 mM NaCl. Fixed gels were incubated in the dark for 10 minutes at room temperature, followed by two washes in PBS and incubation with Hoechst 33342(1 μ g/mL, Invitrogen H3570). Imaging of Nile Red was performed using an Ex/Em of 488nm/530nm and 565nm/600nm. Images were obtained on a Leica TCS SP5 Resonant Scanner with Leica LAS AF software, equipped with 63X/1.40 water UV optimized lens.

Vaginal Smears

Vaginal Smears were performed using 50 μ l ddH₂O, and allowed to dry on the slide. Once dry, the smears were stained with Crystal Violet solution (Sigma) for 1 minute, followed by a one-minute wash in water. Slides were dried and mounted in permount. Smears were visualized on a Leica LMD 7000 mounted with Leica CD310 digital camera using LASV3.7 (Leica) software.

Immunohistochemistry

Tissues were fixed in 10% formalin and washed with PBS prior to dehydration in Leica ASP300S, followed by embedding in paraffin in accordance with standard procedures. Sections were stained for human cMyc (Cell Signaling 5605s), FASN (Abcam ab128856), ADFP (adipophilin)(Abcam ab78920), Phospho-Histone 3 (ser10)(Cell Signaling 9701), BrdU (Abcam ab6326), 8-OHdG Antibody (15A3) (Santacruz sc-66036), PPAR gamma (Invitrogen PA3-8218). Images were obtained on a Leica LMD 7000 mounted with Leica CD310 digital camera using LASV3.7 (Leica) software.

Real-Time Quantitative PCR

Total RNA was extracted from cells using Trizol (Invitrogen). cDNA preparation, including DNase digestion, was performed using QuantiTek(Qiagen) kit starting with 200 ng RNA. Amplifications were run using technical duplicated and biological triplicates in a LightCycler 480 (Roche). Values were adjusted using β -Actin as a reference.

<i>cMYC</i>	5'AGATGGTGACCGAGCTGCTGG3' 5'AAGCCGCTCCACATACAGTC3'
<i>KRASG12D</i>	5'AAGGACAAGGTGTACAGTTATGTGA3' 5'CTCCGTCTGCGACATCTTC3'
<i>NEU</i>	5'TGTACCTTGGGACCAGCTCT3' 5'GGAGCAGGGCCTGATGTGGGTT3'
β -Actin	5'GCTTCTTTGCAGCTCCTTCGT3' 5'ACCAGCCGCAGCGATATCG3'

Western Blot Analysis

Tissue was collected, ground under IN2 and lysed (0.5% Sodium deoxycholate, 25mm Hepes, pH7.5, 150 mm NaCl, 1% Triton-X-100, 0.1% SDS, 5% glycerol, 2mm EGTA). The resulting lysates were subjected to western blotting onto PDVF and stained with anti-FASN (Abcam ab128856 (1:1000)), anti-SREBP1(abcam ab3259 (1 ug/ml), total OXPHOS Rodent WB Antibody Cocktail (Abcam ab110413 6µg/ml), anti-OGG1/2 (Santa-Cruz sc-12075 (1:200)) and Anti- α -Tubulin (Sigma T6199 (1:1000)). After washing with 0.1% Tween-20/TBS, membranes were incubated with HRP conjugated secondary antibodies and developed using the ECL kit (Amersham) after subsequent washing. The signal was read on a Chemidoc XRS (BioRad) and the image processing used Image Lab software.

Quantitative Analysis of BER intermediates using Aldehyde Reactive Probe and Dot-Blot analysis

As previously published (7, 8) DNA was purified from mammary glands isolated from regressed and age matched controls using Blood and Tissue Kit from Qiagen and quantified using Nano-Drop. 1 µg purified DNA was re-suspended in 100µL and incubated with 1mM ARP for 10 minutes at 37°C. After precipitation with cold ethanol, the DNA was resuspended in Tris_EDTA buffer, and re-quantified. 5ng of DNA was heat denatured at 100°C for 5 minutes, quickly chilled on ice, and mixed with an equal amount of 2M ammonium acetate. The DNA was then blotted onto Immobilon-N (Millipore) membrane and UV crosslinked. The membrane was then pre-incubated with a blocking mixture (20 mm Tris-HCl (pH 7.5), 0.1 m NaCl, 1mm EDTA, 0.5% casein, 0.25% BSA, and 0.1% Tween20, pH 7.5) for one hour. The membrane was then incubated in the same buffer containing Steptavidin-conjugated Horseradish Peroxidase (Vector) at room temperature for 30 minutes. The membrane was rinsed 3 times for 10 minutes each in washing buffer (0.26 m NaCl, 1 mm EDTA, 20 mm Tris-HCl, and 0.1% Tween20, pH7.5). The

ARP was then visualized using ECL reagents (Amersham) on a Chemidoc XRS (BioRad) image processing using Image Lab and ImageJ software. Number of biological replicates for analysis (n=4/3) was set to allow for statistical testing.

Modified Comet Assay

The comet assay was performed as previously published (9). Briefly, primary mammary epithelial cells were isolated from regressed and age matched control mice. Following dissection of the mammary gland as outlined previously, epithelial cells were selected on collagen-coated plates. Following selection, cells were trypsinized and dispersed into PBS. Glass slides were precoated in 1% standard agarose (Sigma) and allowed to set. At which point, the previously collected cells were seeded onto the slides in 1% LMP Agarose and covered with an 18 x 18 mm coverslip. They were allowed to set at 4°C for 5 minutes, after which cells were lysed in cold lysis solution (2.5 m NaCl, 0.1 m EDTA, 10 mM Tris, pH 10). Slides were washed in digestion buffer (40 mM HEPES, 0.1 m KCl, 0.5 mM EDTA, 0.2 mg/mL BSA, pH8.0) followed by enzymatic digestion with 1:5,000 dilution of FPG (NEB) diluted in digestion buffer at 37°C for 30 minutes. Slides then underwent alkaline treatment (0.3 m NaOH, 1 mM EDTA) followed by electrophoresis and neutralization (0.4 m Tris, pH 7.5). The slides were then stained with Hoescht and imaged at a Leica LMD 7000 mounted with a Leica CD345FX digital camera using LAS AF software.

Mitochondrial Oxidative Flux

Mitochondrial oxidative flux was determined as previously reported(10). Briefly, 0.4 μ Ci 1-¹⁴C Palmitate (Perkin Elmer) per reaction was evaporated under vacuum and heat followed by resolubilization with Fatty Acid Free BSA for one hour at 60°C. Non-radiolabelled sodium palmitate was also pre-conjugated to fatty acid free BSA at a ratio of 1 mM Sodium

Palmitate/0.17 mm BSA solution(6:1 molar ratio Palmitate:BSA) in order to increase total substrate concentrations to 100 uM. Mitochondria were isolated from regressed mammary glands through homogenization in STE (0.25 m sucrose, 10 mm Tris, 1 mm EDTA). The crude homogenates were spun and the supernatant containing crude mitochondria was used for (1) quantification via Bradford (2) reaction. Twenty µl of crude extract were added to the reaction mixture (0.4 µCi 1-14CPalmitate, 100 uM Palmitate:BSA, 100 mm sucrose, 10 mm Tris-HCl, 5 mm KH₂PO₄, 0.2 mm EDTA, 5 mm NAM, 1 m TSA, 0.3% fatty acid-free BSA, 80 mm KCl, 1 mm MgCl₂, 2 mm L-carnitine, 0.1 mm malate, 0.05 mm coenzyme A, pH 8.0), and incubated for 60 minutes at 37 C. The reaction was then transferred to Eppendorf tubes containing 1 m Perchloric Acid, and released CO₂ was captured on NaOH soaked whatman filter disks placed in the caps for one hour at room temperature. Following which the whatmann filters were placed in scintillation fluid and counted at PERKIN ELMER X liquid scintillation counter. While the reaction mixture was spun down to precipitate the non-oxidized palmitate, the supernatant containing acid soluble metabolites was then counted in scintillation fluid. Number of biological replicates for analysis (n=3 for controls and n=4 for experimental animals) was set to allow for statistical testing.

Cell Collection for intracellular and extracellular metabolomic analysis

Matrigel was digested for 1,5 h in order to free the organoids. Organoids were pooled from 6-wells of a 12-well plate and washed thrice with PBS followed by short centrifugation steps (1000 rpm, 2 min). Organoids were finally quenched by adding 200ul cold (-80°C) HPLC-grade methanol (Biosolve Chimie, France). 50µl of the spent growth medium of each well and the last washing solution of each sample were also collected and quenched with 100µl of cold (-80°C)

HPLC-grade methanol (Biosolve Chimie, France). Comparison between the metabolic profiles of these liquids enables the validation of the effective cell washing before quenching.

Metabolomic Data Acquisition

The dried polar metabolite extracts of the organoids were obtained based on the methanol/water protocol, which is described in (11, 12) and (13), with ribitol (Alfa Aesar, UK) added as internal standard. The dried extracts were derivatized to their (MeOx)TMS-derivatives through reaction with 50 μ L of 20 mg/mL methoxyamine hydrochloride (Alfa Aesar, UK) solution in pyridine (Sigma-Aldrich) for 90 min at 40°C, followed by reaction with 100 μ L N-methyl-trimethylsilyl-trifluoroacetamide (MSTFA) (Alfa Aesar, UK) for 12 hours at room temperature, as justified in (13) and (14). The metabolic profile of each sample was measured at 12 hours post-derivatization, using a Shimadzu TQ8040 GC-(triple quadrupole) MS system (Shimadzu Corp.). The gas chromatograph was equipped with a 30m x 0.25 mm x 0.25 μ m DB-50MS capillary column (Phenomenex, USA). The detector was operated both in scan mode recording in the range of 50-600 m/z, as well as in MRM mode for the following fatty acids: myristate, palmitate, stearate, oleate, elaidic acid and cholesterol.

Expression Profiling on Organoids: MIAME checklist

Goal of the experiment. To profile gene expression of in vitro cultured primary mouse mammary cells pre-, during, and post- oncogene induction.

Description of experiment. Mammary glands from 8 week old, female, virgin GEMM *TetO-cMYC/TetO-Neu(HER2)/MMTV-rtTA* and *TetO-cMYC/TetO-Kras^{G12D}/MMTV-rtTA* mice were dissociated into single cells and seeded into matrigel matrix for in vitro culture. To determine the gene expression changes which occur upon oncogene induction 5 days after seeding, doxycycline was added to the media for 5 days, and then removed. Samples were taken of the

following populations: 5 days on, 5 days on/7days off and never induced. Number of biological replicates for analysis (n=3) was set to allow for statistical testing.

Keywords. MYC, NEU, KRAS^{G12D}, primary mammary epithelium

Experimental Design. Total RNA was extracted for each group in 3 independent organoid experiments. Gene expression profiles were determined for the MYC/KRAS dataset using the MoGene1.0-st-v1 platform from Affymetrix. Gene expression profiles were determined for the MYC/NEU dataset using the MoGene2.0-st platform from Affymetrix.

Quality Control. Total RNA was quality checked using Bioanalyser All samples had an RNA integrity number > 9.

Public databases. All data files can be accessed through the ArrayExpress (accession number E-MTAB-3038) and (accession number E-MTAB-3039).

Origin of each sample. 8-week-old, female, virgin GEMM (*TetO-cMYC/TetO-Neu(HER2)/MMTV-rtTA* and *TetO-cMYC/TetO-Kras^{G12D}/MMTV-rtTA* mice) in FVB background.

Manipulation of samples. Mammary glands were dissociated in collagenase and liberaseTM for 14-16h at 37°C, treated with trypsin, DNase, and seeded into matrigel matrix. Cells were cultured in MEBM media at 37°C in a 5%(vol/vol) CO₂ atmosphere. The media was supplemented with Doxycycline where appropriate at a final concentration of 1 µg/mL.

RNA preparation method for all samples. Total RNA was extracted using TRIZOL(Invitrogen) following manufacturer's instructions for all samples.

Experimental factor values. Cell type: Mouse mammary epithelial cells, never induced, cultured in the presence of doxycycline for 5 days, cultured in the presence of doxycycline for 5 days, with subsequent 7 days additional culture following doxycycline removal.

Amplification method. Biotinylated cDNA was synthesized from total RNA using Ambion WT Expression kit (#4491974)

cDNA hybridization and Stain: Following fragmentation and labeling (WT terminal Labeling and Controls Kit, Affymetrix, #901524), cDNA was hybridized for 16 hr at 37C on GeneChip Mouse Gene 1.0 ST Array or GeneChip Mouse Gene 2.0 ST Array. GeneChips were washed and stained in the Affymetrix Fluidics Station 450.

Platform. Affymetrix murine MoGene1.0-st-v1 and MoGene2.0-st platforms. **Sample name.** NeverInduced

Description. RNA extracted from primary mouse mammary epithelial cells cultured in matrigel matrix. Cells were maintained in MEBM for the length of the experiment, 17 days.

Sample name. 5DayON

Description. RNA extracted from primary mouse mammary epithelial cells cultured in matrigel matrix. Cells were maintained in MEBM for 5 days and then in media supplemented with 1 µg/mL doxycycline for an additional 5 days, at which time RNA was harvested.

Sample name. Regressed

Description. RNA extracted from primary mouse mammary epithelial cells cultured in matrigel matrix. Cells were maintained in MEBM for 5 days and then in media supplemented with 1 µg/mL doxycycline for an additional 5 days before then replacing the media with doxycycline free MEBM for an additional 7 days, at which time RNA was harvested.

Sample name. NeverInduced

Description. RNA extracted from primary mouse mammary epithelial cells cultured in matrigel matrix. Cells were maintained in MEBM for the length of the experiment, 17 days.

Microarray Data Processing

Array data analysis was carried out using R with Bioconductor packages oligo, limma and XML. Datasets were background corrected and normalized using the Robust Multichip Average (RMA) algorithm provided by oligo (15). Quality control of both the raw and the normalized data was performed using the Bioconductor package arrayQualityMetrics.

Processing of the MoGene arrays, as well as the re-analysis of the HG-U133A microarray data (GEO accession number GSE32072) was performed using the RMA algorithm of the Bioconductor package oligo and associated array annotation databases. Reannotated databases for MoGene arrays were produced with a custom R script matching the original Affymetrix probe definitions to updated gene definitions of the Ensembl Reference Genome (build m38.p4, release 82). For the GSE32072 brainarray ENSG annotation, version 19.0.0, was used(16). Differential expression analysis was performed using limma. The resulting p-values were corrected for multiple-testing using the BH algorithm (17) and a false discovery rate (FDR) cutoff of 5% was chosen.

Unified processing of Myc/Kras and Myc/Neu arrays

Expression data from MYC/KRAS (array type MoGene-1) and MYC/NEU (array type MoGene-2) perturbations were processed together retaining only the intersection of the datasets, i.e. only keeping the expression values for the genes present in both array annotation databases. The Variance Stabilisation and Normalisation technique in combination with Surrogate Variable Analysis with n=1 surrogate variables were used to adjust for the batch effect of different array platforms. For this, the Bioconductor packages vsn and sva were utilized(18, 19).

Analysis of Human RNA-Seq Data

The single-end reads were mapped to the GRCh38 reference genome obtained from ENSEMBL 82 using STAR 2.5.1a with default settings(20). Mapped reads overlapping exons as annotated in

the ENSEMBL 82 gtf-file were summarized to gene level count tables by STAR. Since the alignment strand was opposite of the genomic feature strand, we used the “reverse” count tables returned by STAR. We then used DESeq2 1.10.1 to import the count data into R(21). Since differences between the samples that could not be normalized using a simple scaling method with one factor per sample were present, we used the cyclic loess method to compute gene-specific normalization factors for each sample. Specifically, the function normOffsets from the Bioconductor package csaw was used to obtain these factors, which were then exponentiated and used as normalization factors in the DESeq analysis (22, 23).

A PCA analysis revealed a sample switch for patient 207: most probably the post and pre-treatment samples were switched. We thus changed their group labels accordingly. Finally, a regularized logarithm transformation available in DESeq2 was performed on the data (a more sophisticated logarithmic transformation). All data files can be accessed through the ArrayExpress "Expression RNA-Seq data of matched cases of pre-treatment Fine-needle aspiration (FNA) and the respective post neo-adjuvant treatment operative sample of breast cancer patients" which has been assigned ArrayExpress accession E-MTAB-4632.

Pathway and Metabolite Enrichment Analysis

Enrichment analysis of REACTOME pathways was performed after removal of the stromal signature gene list of Gonzalez-Angulo et al.(24) from the human data sets GSE32072 and E-MTAB-4632. REACTOME is organized hierarchically with 24 large aggregates at the top level which cannot provide meaningful pathway enrichment overviews. Three top levels with all their enclosed subpathways were unrelated to the current study and were excluded: “Muscle contraction”, “Hemostasis”, “Reproduction”; For the remaining 21 generic REACTOME top level aggregates, serving as unions of more specific pathways, such as “Metabolism”, “Disease”

or “Cell-Cell communication” were excluded: However all enclosed lower level pathways were included in the enrichment analysis. Both microarray and RNA-seq data enrichments were conducted with the “reporter” method of the Bioconductor package piano(25, 26). Gene set statistics of the distinct-directional class pDistinctDirup were utilized, in order to capture the pathways significantly affected by upregulation in pathway gene expression, but not downregulation, or a mix of up- and downregulation. To account for difference in sensitivity of the analysis for the mouse organoid cultures and human clinical samples, p-value significance levels of 0.005 and 0.05 were used for KRAS/NEU and GSE32072/ RNA-seq data correspondingly. Gene sets that contain less than 3 genes were excluded from the analysis.

The overlaps of significant pathways between the KRAS/NEU data, GSE32072 and RNA-seq data were determined.

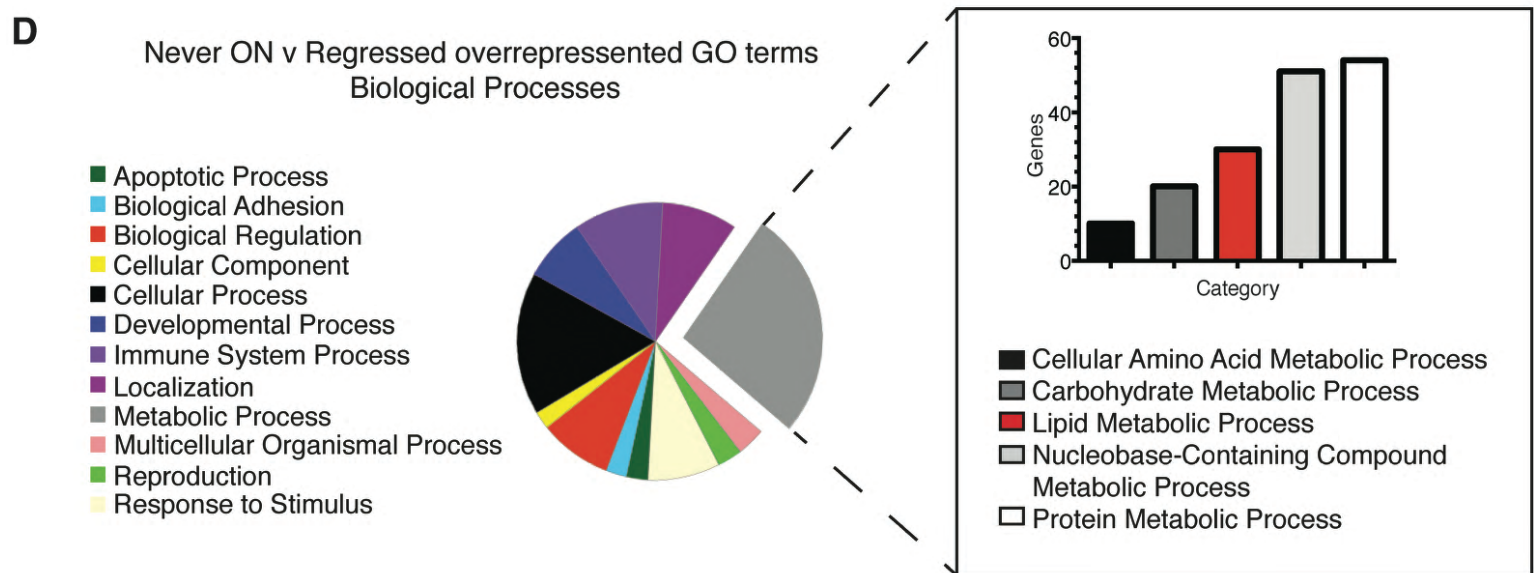
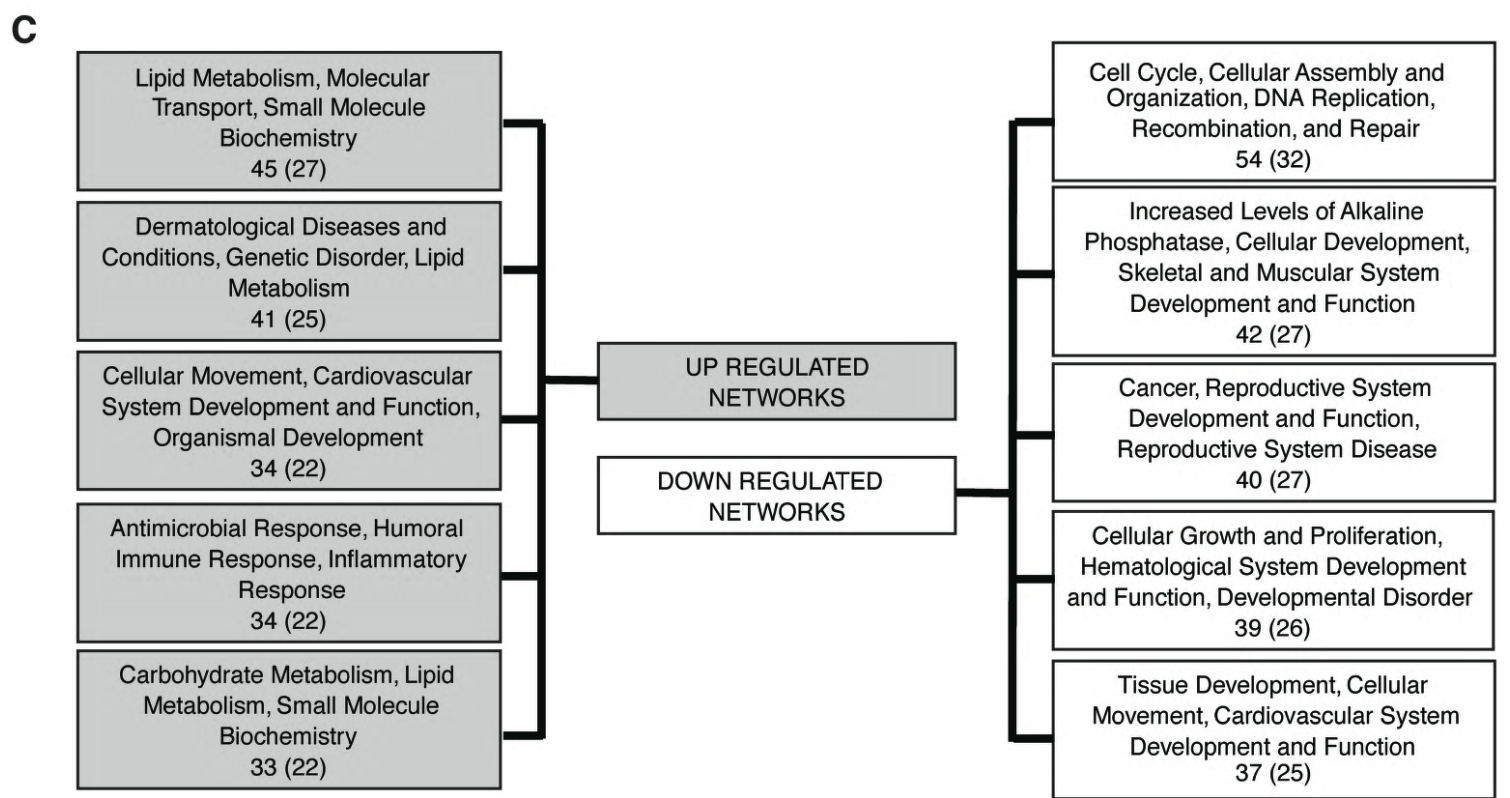
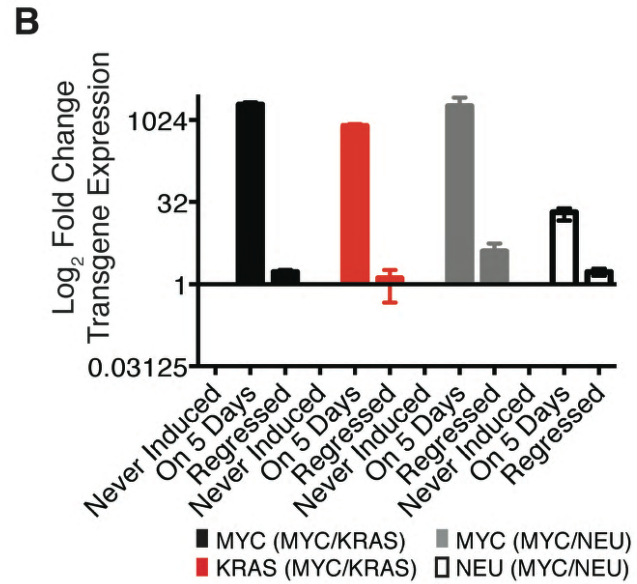
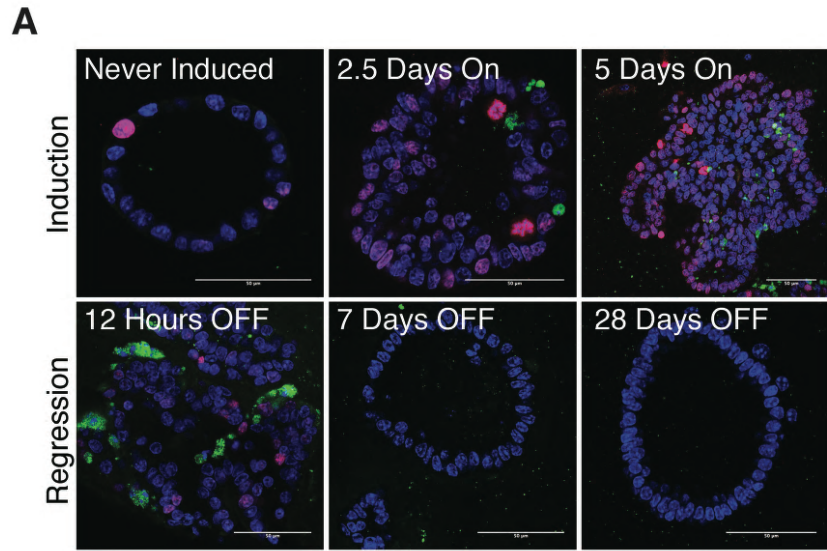
Metabolite Enrichment: Reporter metabolites were calculated as previously described (25, 26). Briefly, each metabolite in a mouse genome-scale metabolic reconstruction (see below) was scored for significance of enrichment in transcriptional changes in its neighboring enzymes. As with the pathway analysis above, pDistinctDirup statistics from the “reporter” method in the piano Bioconductor package were obtained. A p-value significance level cut-off was set to 0.005 for KRAS/NEU data sets and 0,05 for GSE32072/ RNA-seq data sets. Gene sets with less than 3 genes were excluded from the analysis. A statistically significant score suggests altered concentration of, and/or, flux through the corresponding metabolite.

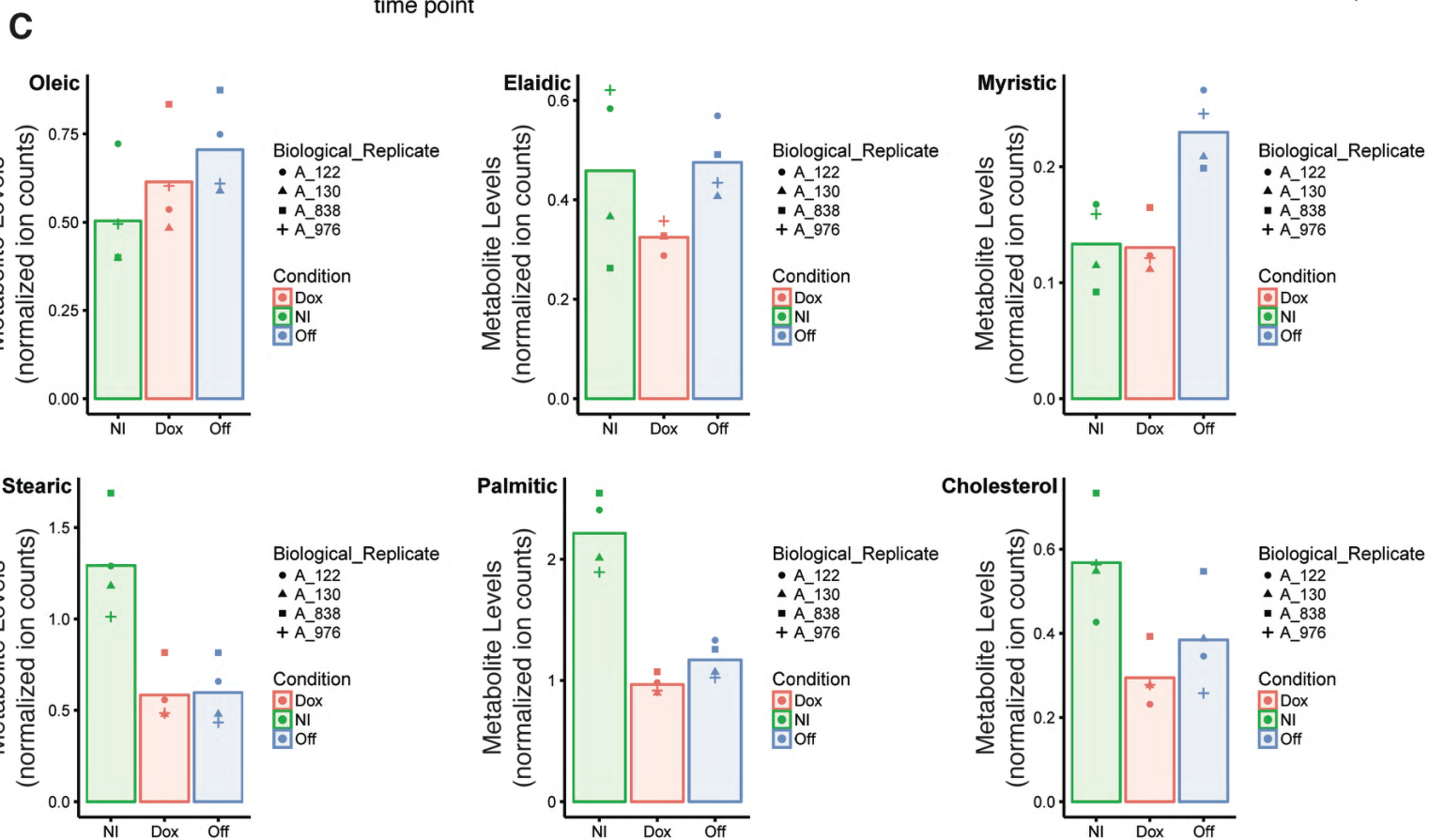
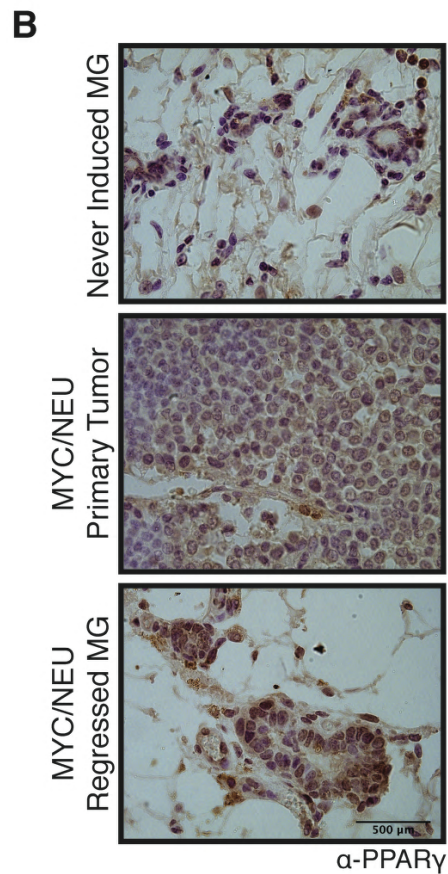
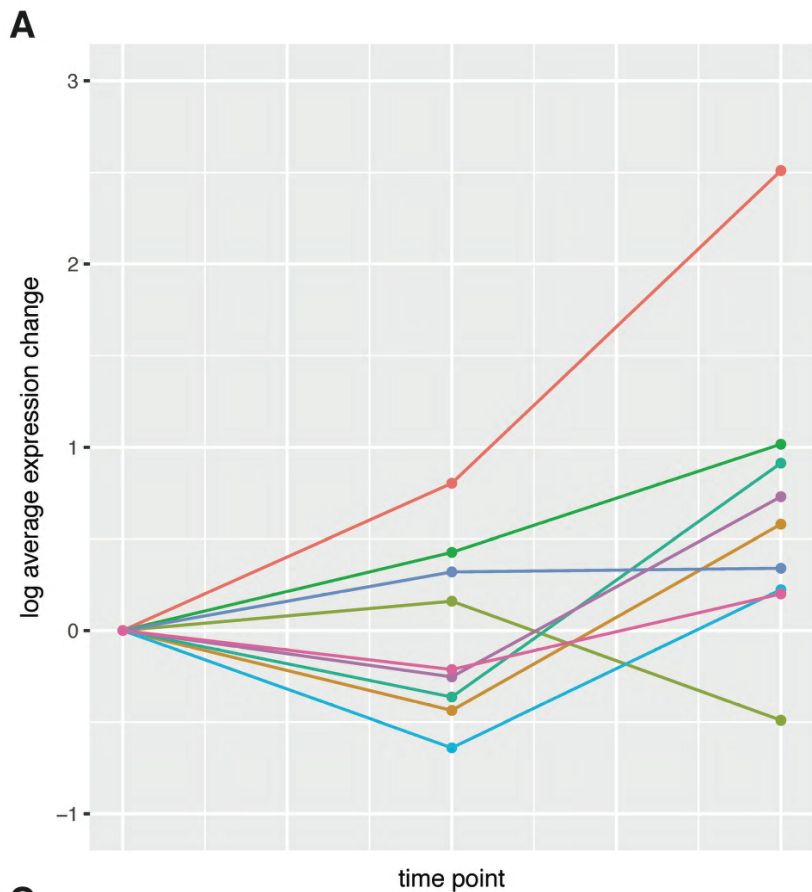
Mouse genome-scale metabolic model: We used an unpublished model, provided by J. Nielsen (Chalmers University). In essence, the model was ‘translated’ from the human Recon-2 model(27) using (sequence) homology-based mapping between human and mouse genes. This

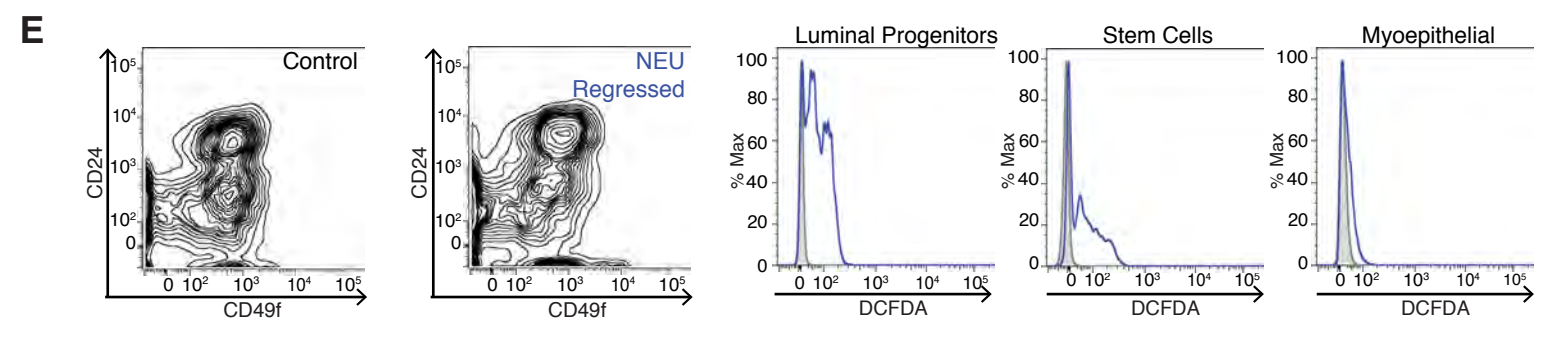
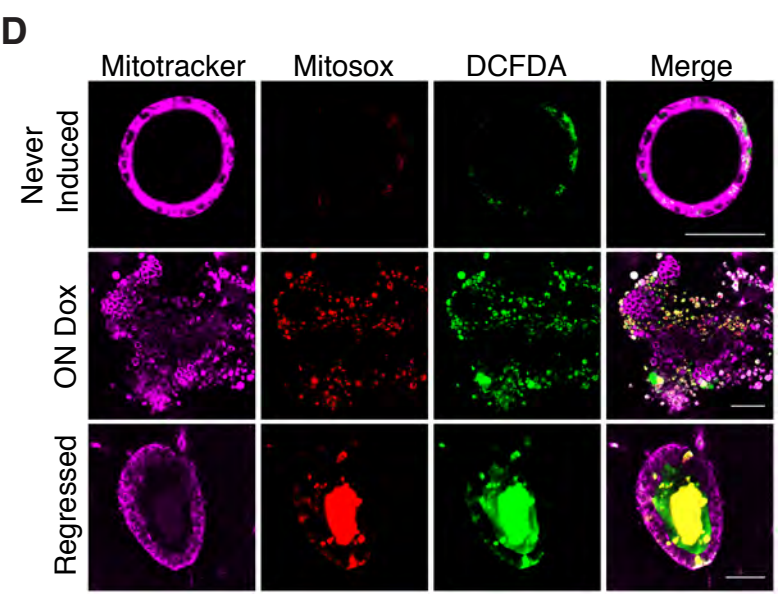
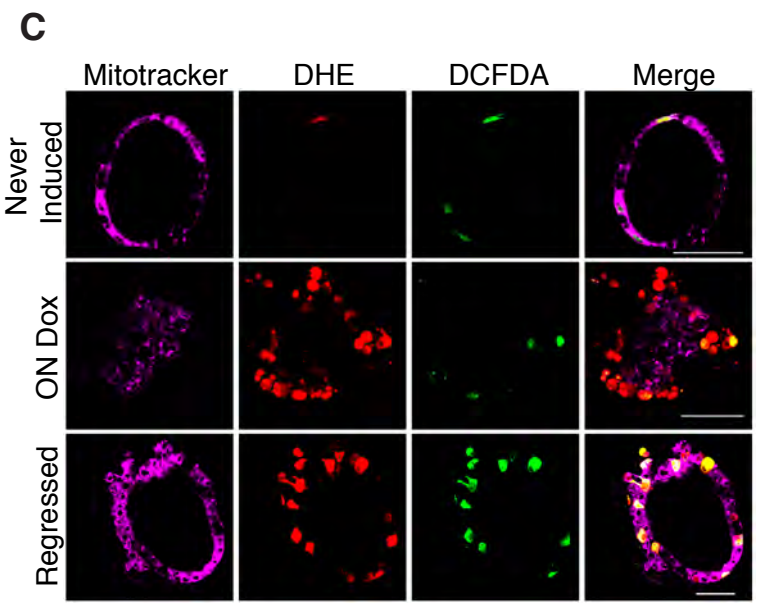
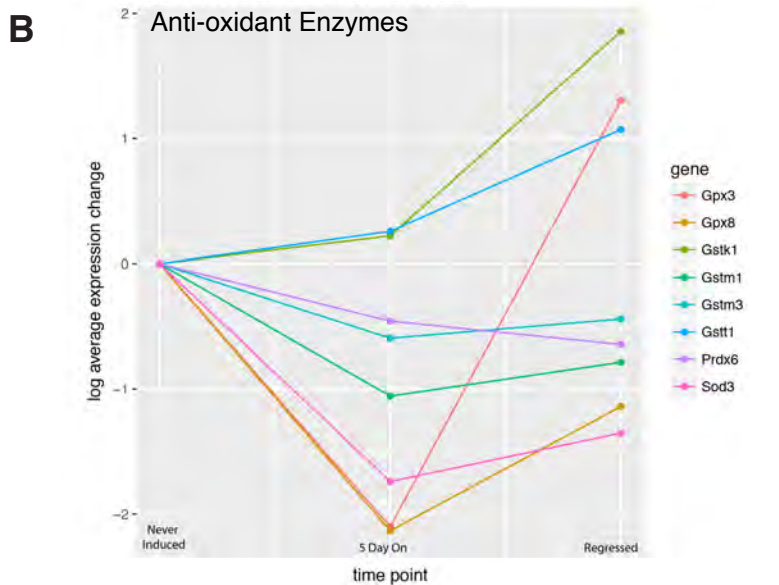
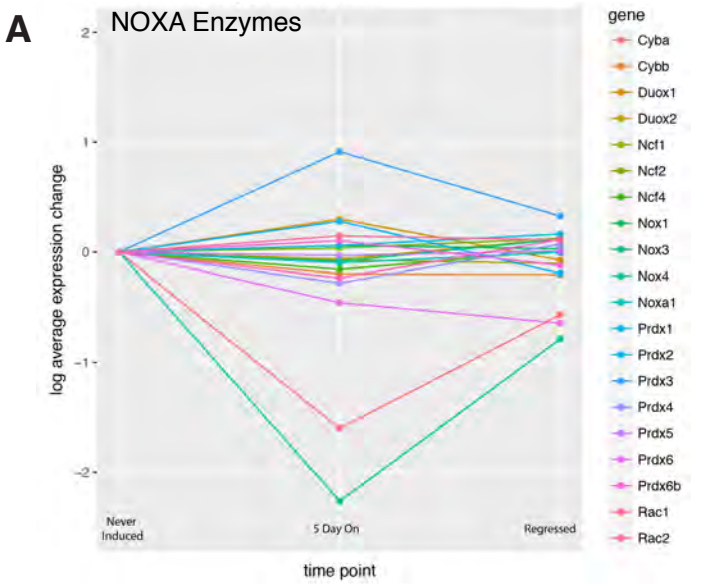
homology model was then manually corrected to address a few known issues regarding the gene-reaction mappings in the human model.

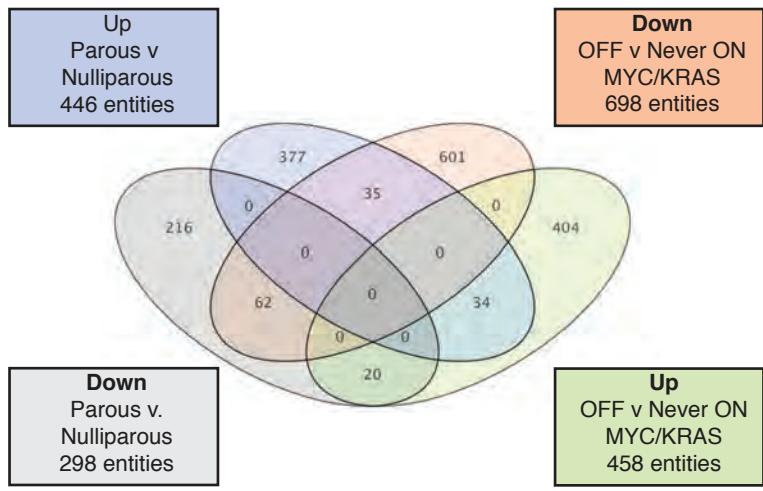
1. Gyori BM, Venkatachalam G, Thiagarajan PS, Hsu D, and Clement MV. OpenComet: An automated tool for comet assay image analysis. *Redox biology*. 2014;2(457-65).
2. Teta M, Rankin MM, Long SY, Stein GM, and Kushner JA. Growth and regeneration of adult beta cells does not involve specialized progenitors. *Developmental cell*. 2007;12(5):817-26.
3. Jechlinger M, Podsypanina K, and Varmus H. Regulation of transgenes in three-dimensional cultures of primary mouse mammary cells demonstrates oncogene dependence and identifies cells that survive deinduction. *Genes & development*. 2009;23(14):1677-88.
4. Shackleton M, Vaillant F, Simpson KJ, Stingl J, Smyth GK, Asselin-Labat ML, Wu L, Lindeman GJ, and Visvader JE. Generation of a functional mammary gland from a single stem cell. *Nature*. 2006;439(7072):84-8.
5. Stingl J, Eirew P, Ricketson I, Shackleton M, Vaillant F, Choi D, Li HI, and Eaves CJ. Purification and unique properties of mammary epithelial stem cells. *Nature*. 2006;439(7079):993-7.
6. Listenberger LL, and Brown DA. Fluorescent detection of lipid droplets and associated proteins. *Current protocols in cell biology / editorial board, Juan S Bonifacino [et al]*. 2007;Chapter 24(Unit 24 2).
7. Nakamura J, and Swenberg JA. Endogenous apurinic/apyrimidinic sites in genomic DNA of mammalian tissues. *Cancer research*. 1999;59(11):2522-6.
8. Nakamura J, Walker VE, Upton PB, Chiang SY, Kow YW, and Swenberg JA. Highly sensitive apurinic/apyrimidinic site assay can detect spontaneous and chemically induced depurination under physiological conditions. *Cancer research*. 1998;58(2):222-5.
9. Collins AR, and Dusinska M. Oxidation of cellular DNA measured with the comet assay. *Methods in molecular biology*. 2002;186(147-59).
10. Hirschey MD, Shimazu T, Goetzman E, Jing E, Schwer B, Lombard DB, Grueter CA, Harris C, Biddinger S, Ilkayeva OR, et al. SIRT3 regulates mitochondrial fatty-acid oxidation by reversible enzyme deacetylation. *Nature*. 2010;464(7285):121-5.
11. Chrysanthopoulos PK, Goudar CT, and Klapa MI. Metabolomics for high-resolution monitoring of the cellular physiological state in cell culture engineering. *Metabolic engineering*. 2010;12(3):212-22.
12. Vernardis SI, Goudar CT, and Klapa MI. Metabolic profiling reveals that time related physiological changes in mammalian cell perfusion cultures are bioreactor scale independent. *Metabolic engineering*. 2013;19(1-9).
13. Kanani HH, and Klapa MI. Data correction strategy for metabolomics analysis using gas chromatography-mass spectrometry. *Metabolic engineering*. 2007;9(1):39-51.
14. Kanani H, Chrysanthopoulos PK, and Klapa MI. Standardizing GC-MS metabolomics. *J Chromatogr B Analyt Technol Biomed Life Sci*. 2008;871(2):191-201.
15. Carvalho BS, and Irizarry RA. A framework for oligonucleotide microarray preprocessing. *Bioinformatics*. 2010;26(19):2363-7.
16. Dai MH, Wang PL, Boyd AD, Kostov G, Athey B, Jones EG, Bunney WE, Myers RM, Speed TP, Akil H, et al. Evolving gene/transcript definitions significantly alter the interpretation of GeneChip data. *Nucleic acids research*. 2005;33(20).

17. Benjamini Y, and Hochberg Y. Controlling the False Discovery Rate: a Practical and Powerful Approach to Multiple Testing. *Journal of the Royal Statistics Society*. 1995;57(1):289-300.
18. Huber W, von Heydebreck A, Sultmann H, Poustka A, and Vingron M. Variance stabilization applied to microarray data calibration and to the quantification of differential expression. *Bioinformatics*. 2002;18 Suppl 1(S96-104).
19. Leek JT, Johnson WE, Parker HS, Jaffe AE, and Storey JD. The sva package for removing batch effects and other unwanted variation in high-throughput experiments. *Bioinformatics*. 2012;28(6):882-3.
20. Dobin A, Davis CA, Schlesinger F, Drenkow J, Zaleski C, Jha S, Batut P, Chaisson M, and Gingeras TR. STAR: ultrafast universal RNA-seq aligner. *Bioinformatics*. 2013;29(1):15-21.
21. Love MI, Huber W, and Anders S. Moderated estimation of fold change and dispersion for RNA-seq data with DESeq2. *Genome biology*. 2014;15(12):550.
22. Lun AT, and Smyth GK. De novo detection of differentially bound regions for ChIP-seq data using peaks and windows: controlling error rates correctly. *Nucleic acids research*. 2014;42(11):e95.
23. Ballman KV, Grill DE, Oberg AL, and Therneau TM. Faster cyclic loess: normalizing RNA arrays via linear models. *Bioinformatics*. 2004;20(16):2778-86.
24. Gonzalez-Angulo AM, Iwamoto T, Liu S, Chen H, Do KA, Hortobagyi GN, Mills GB, Meric-Bernstam F, Symmans WF, and Pusztai L. Gene expression, molecular class changes, and pathway analysis after neoadjuvant systemic therapy for breast cancer. *Clinical cancer research : an official journal of the American Association for Cancer Research*. 2012;18(4):1109-19.
25. Patil KR, and Nielsen J. Uncovering transcriptional regulation of metabolism by using metabolic network topology. *Proceedings of the National Academy of Sciences of the United States of America*. 2005;102(8):2685-9.
26. Zelezniak A, Pers TH, Soares S, Patti ME, and Patil KR. Metabolic network topology reveals transcriptional regulatory signatures of type 2 diabetes. *PLoS computational biology*. 2010;6(4):e1000729.
27. Thiele I, Swainston N, Fleming RM, Hoppe A, Sahoo S, Aurich MK, Haraldsdottir H, Mo ML, Rolfsson O, Stobbe MD, et al. A community-driven global reconstruction of human metabolism. *Nat Biotechnol*. 2013;31(5):419-25.

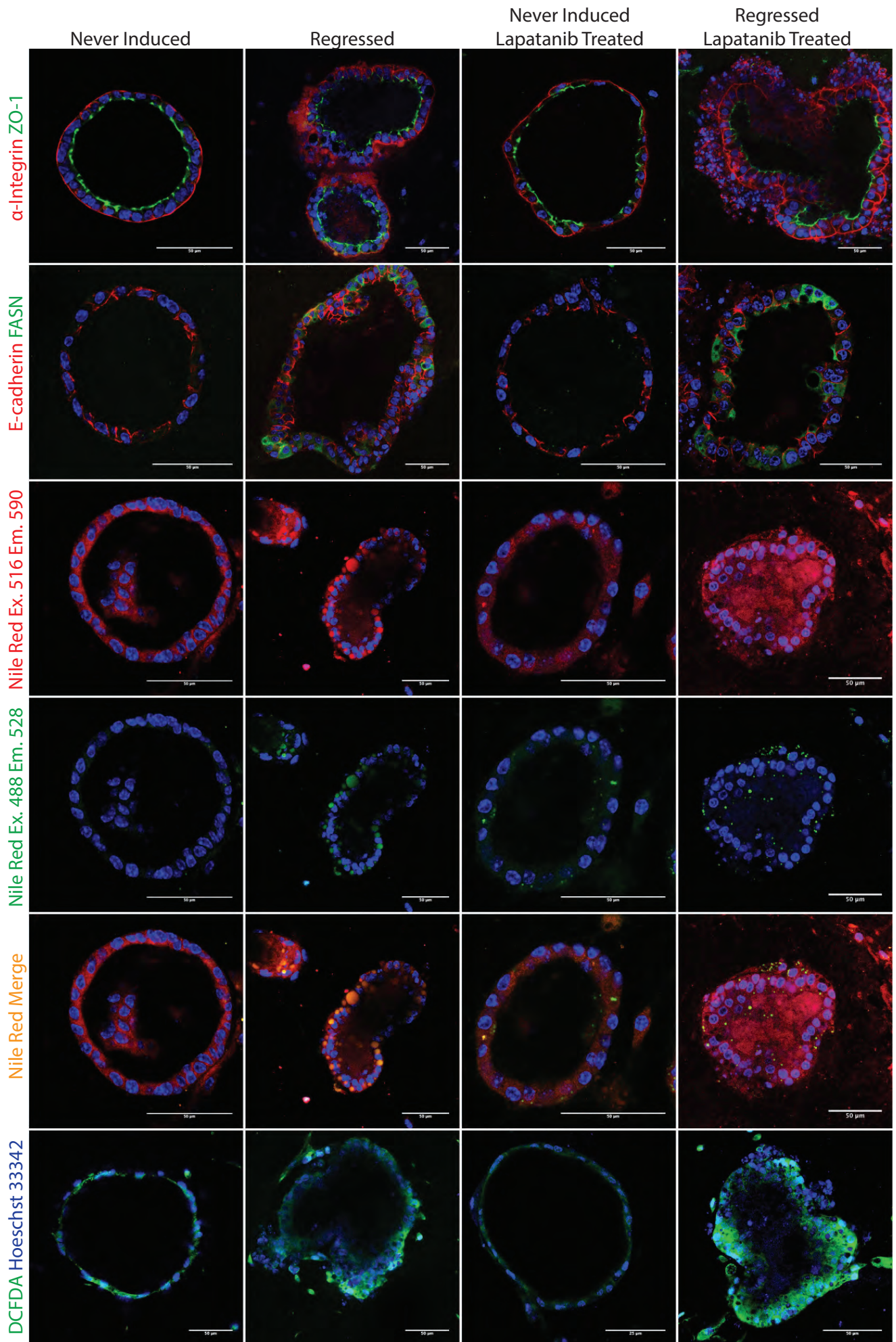


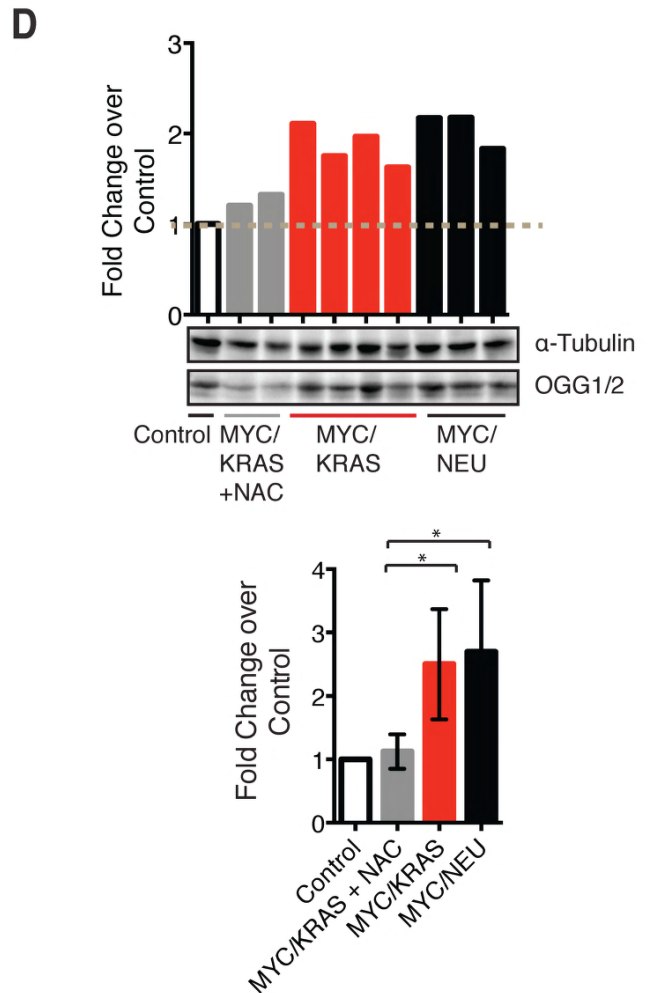
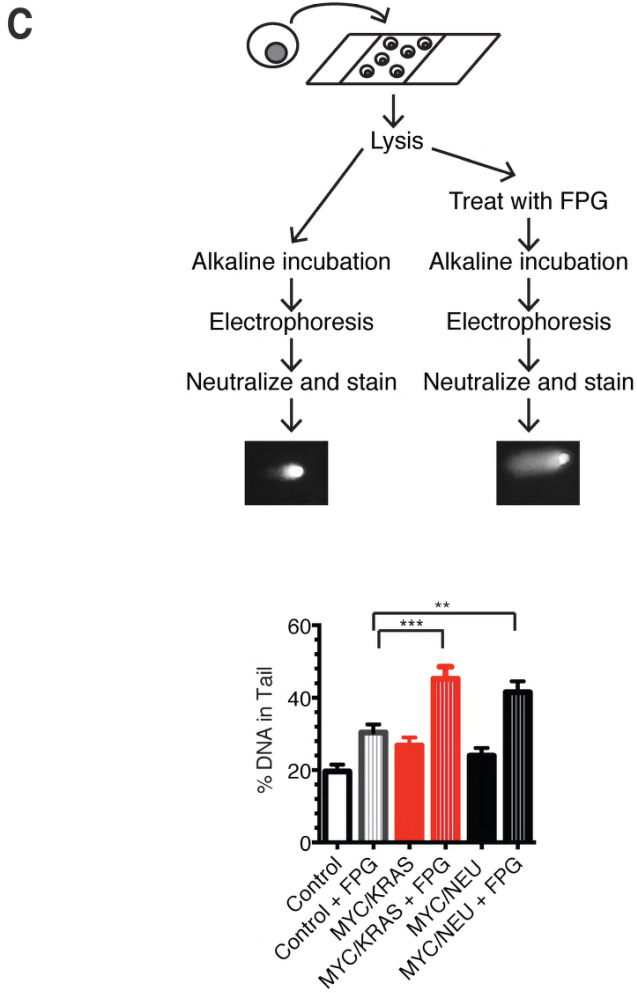
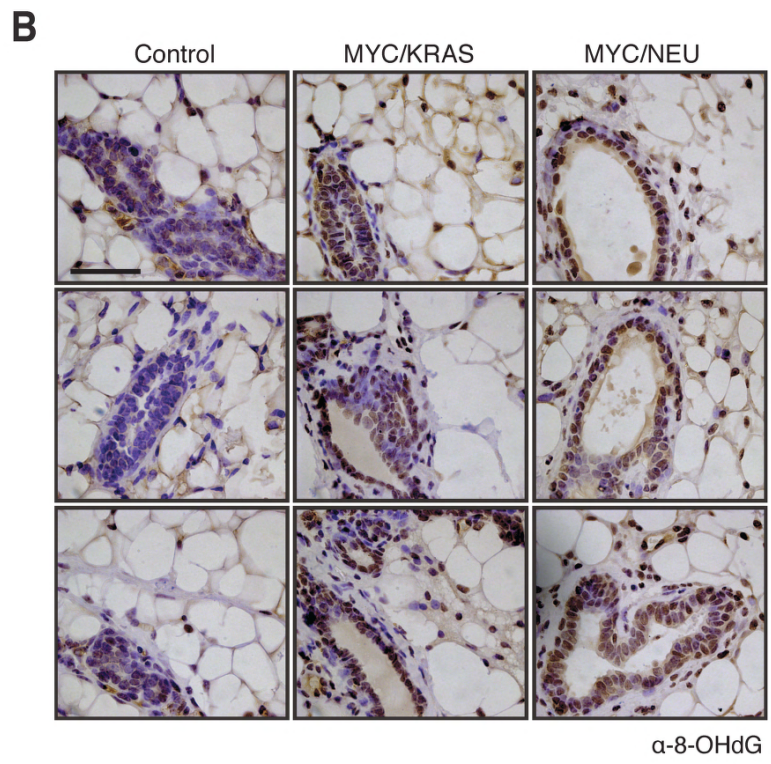
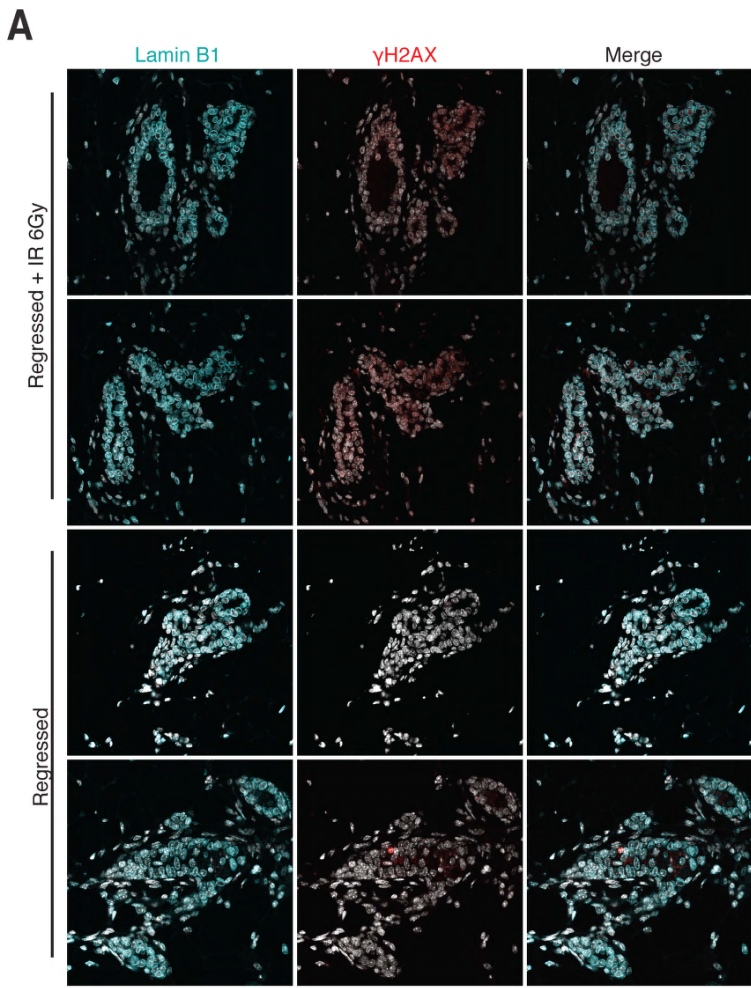


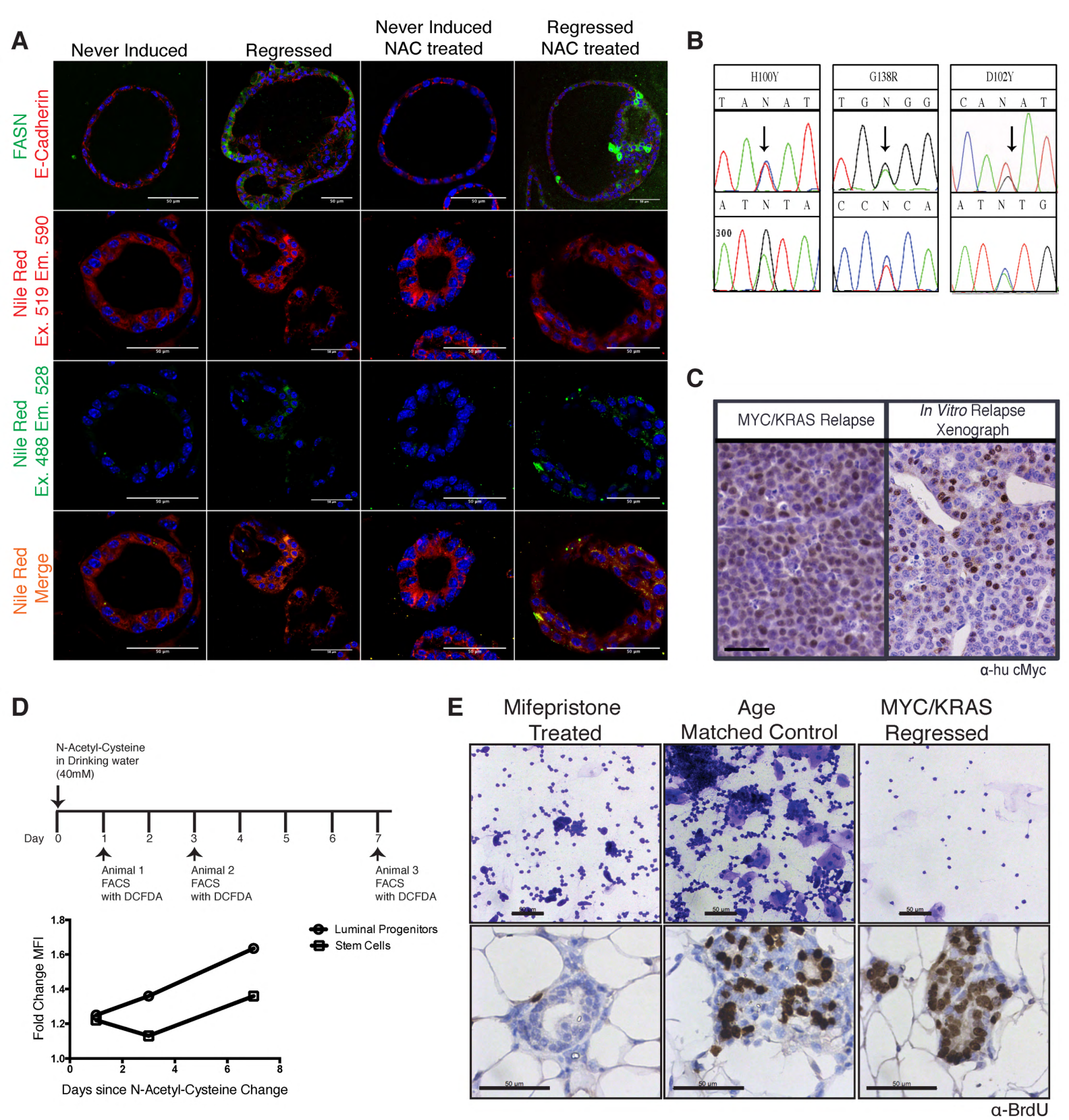


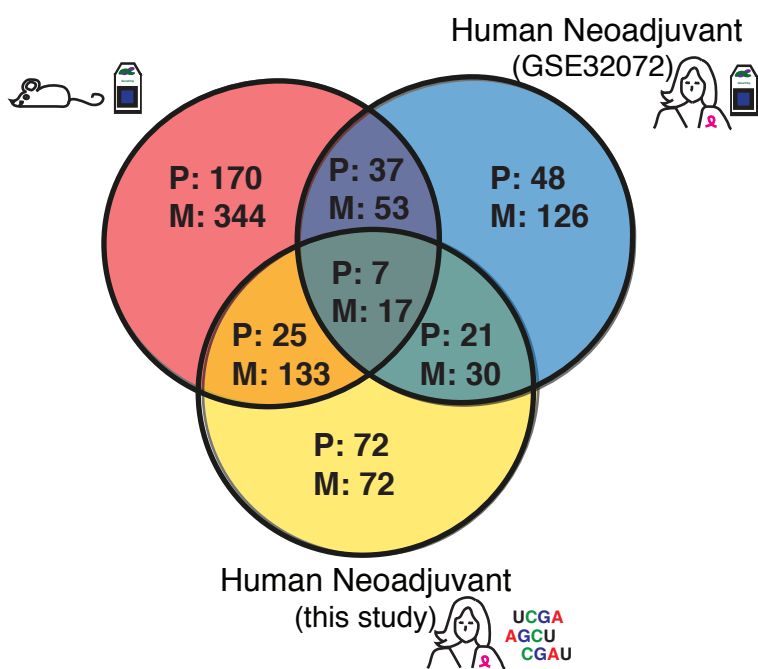
A**B**

<u>MSigDB Gene Set for Up Regulated Genes</u>	<u>P-value</u>
MCBRYAN_PUBERTAL_BREAST_4_5WK_UP	3.23 e ⁻¹⁷
WONG_ADULT_TISSUE_STEM_MODULE	3.61 e ⁻¹⁹
GRAESSMANN_APOPTOSIS_BY_DOXYRUBICIN_UP	2.56 e ⁻¹⁸
PLASARI_TGFB1_TARGETS_10HR_DN	3.91 e ⁻¹⁸
MCBRYAN_PUBERTAL_BREAST_3_4WK_UP	1.71 e ⁻¹⁶
LIN_MAMMARY_STEM_CELL_UP	9.03 e ⁻¹⁶
<u>MSigDB Gene Set for Down Regulated Genes</u>	<u>P-value</u>
DUTERTRE ESTRADIOL_RESPONSE_24HR_UP	2.5 e ⁻³¹
WANG_RESPONSE_TO_GSK3_INHIBITOR_SB216716763_DN	3.68 e ⁻³¹
BERENJENO_TRANSFORMED_BY_RHOA_UP	1.36 e ⁻²⁹
KOBAYASHI_EGFR_SIGNALING_24HR_DN	2.33 e ⁻²⁹









Pathways Mouse/Human GSE32072:

- Membrane Trafficking
- Phospholipid metabolism
- RHO GTPases Activate ROCKs
- Sema4D induced cell migration and growth-cone collapse
- Signaling by NOTCH
- Acyl chain remodeling of DAG and TAG
- Regulation of lipid metabolism by PPARalpha
- Signaling by Hippo

Metabolites Mouse/Human GSE32072:

- O-phosphoprotamine
- ubiquitin
- activation-ppara
- PPARA
- fatty acid-ligands
- 11-carboxy-alpha-tocotrienol
- (2E)-dodecenoyl-CoA
- (2E,6Z,9Z,12Z)-octadecatetraenoyl-CoA

Pathways Intesection Mouse/Human RNA-seq/GSE32072:

- Metabolism of lipids and lipoproteins
- Glycosaminoglycan metabolism
- Heparan sulfate/heparin (HS-GAG) metabolism
- ECM proteoglycans
- HS-GAG biosynthesis
- Chondroitin sulfate/dermatan sulfate metabolism
- Type I hemidesmosome assembly

Metabolites Intesection Mouse/Human RNA-seq/GSE32072:

- UDP
- (8Z,11Z,14Z,17Z)-eicosatetraenoyl-CoA
- (5Z,8Z,11Z,14Z,17Z)-eicosapentaenoyl-CoA
- (6Z,9Z,12Z,15Z)-octadecatetraenoyl-CoA
- (8Z,11Z)-eicosadienoyl-CoA
- (5Z,8Z,11Z)-eicosatrienoyl-CoA
- propanoyl-CoA
- (3Z)-dodecenoyl-CoA

Pathways Mouse/Human RNA-seq:

- Signaling by GPCR
- Sphingolipid metabolism
- O-linked glycosylation
- IL-6-type cytokine receptor ligand interactions
- Molecules associated with elastic fibres
- Biological oxidations
- Regulation of IGF transport and uptake by IGFBPs
- Ephrin signaling

Metabolites Mouse/Human RNA-seq:

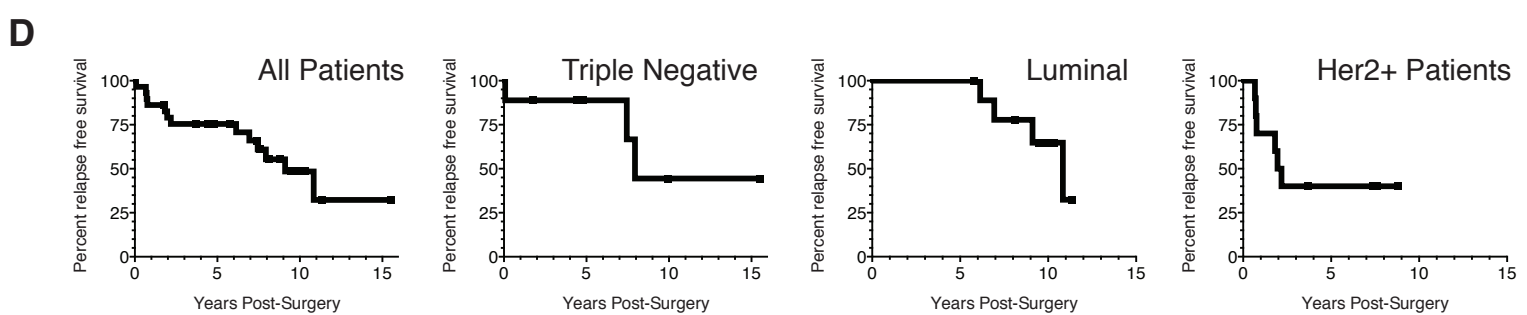
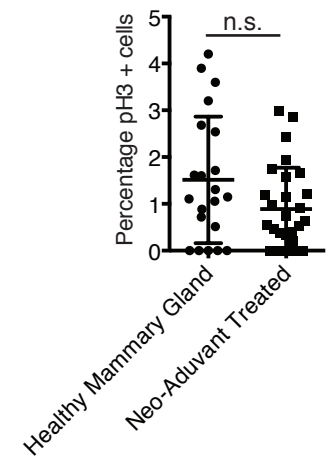
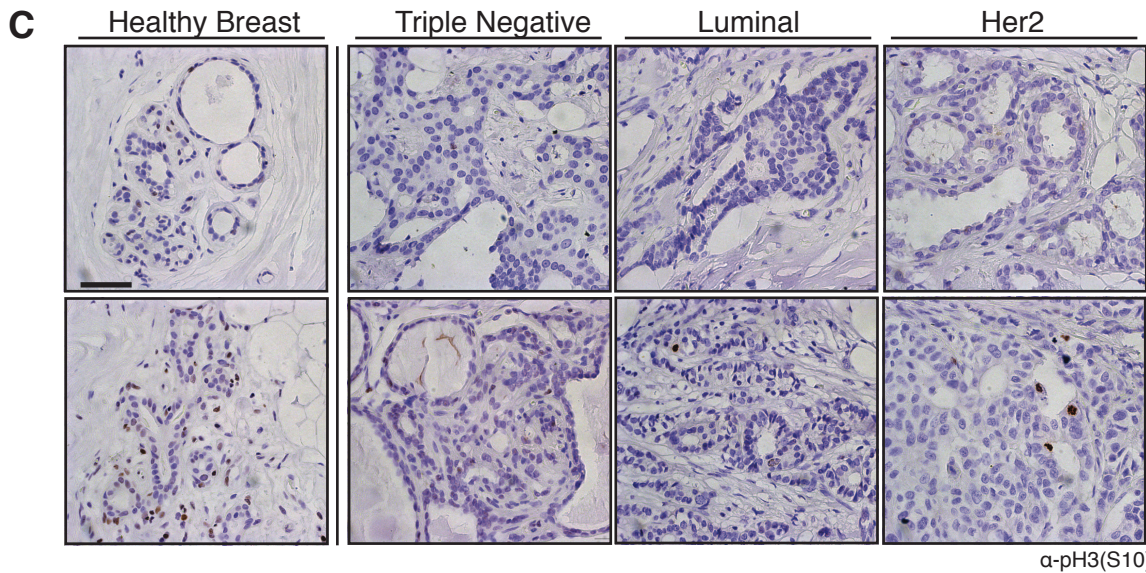
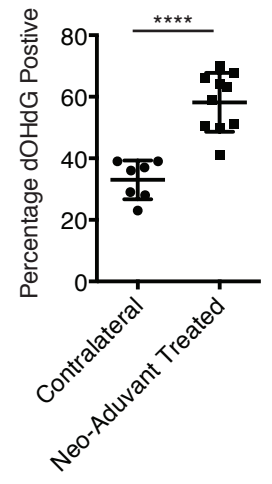
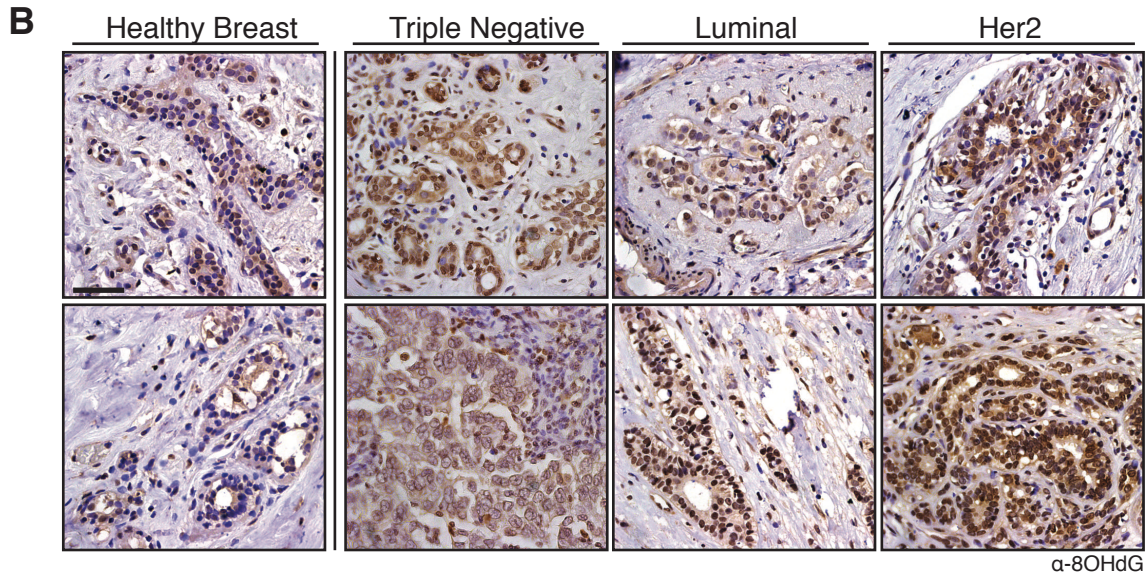
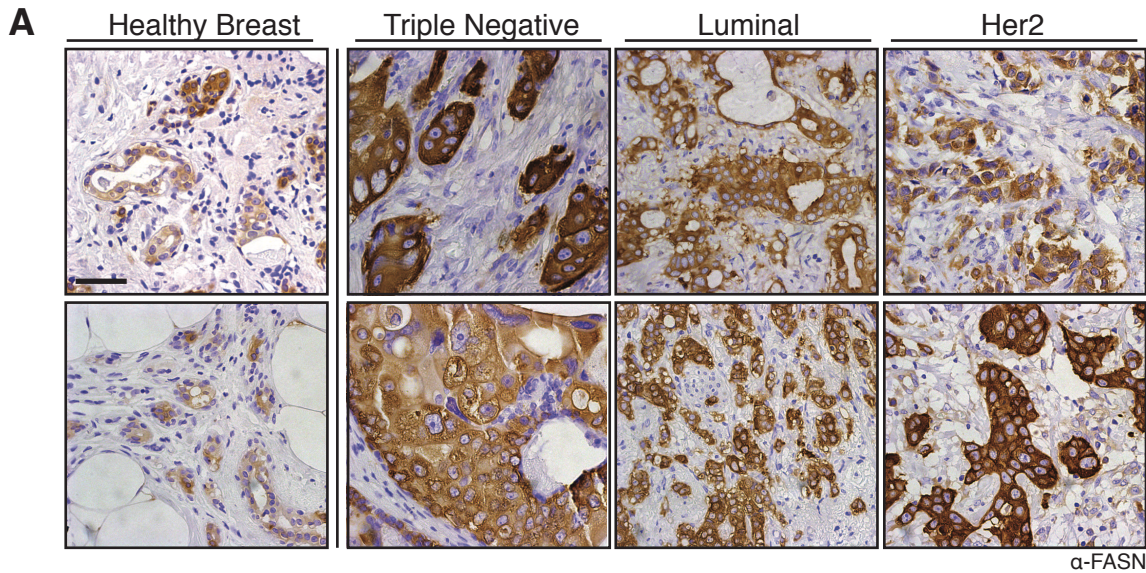
- O2
- arachidonate
- PC-LD pool
- stearoyl-CoA
- (11Z)-eicosenoyl-CoA
- myristoyl-CoA
- cis-vaccenoyl-CoA
- palmitoleoyl-CoA

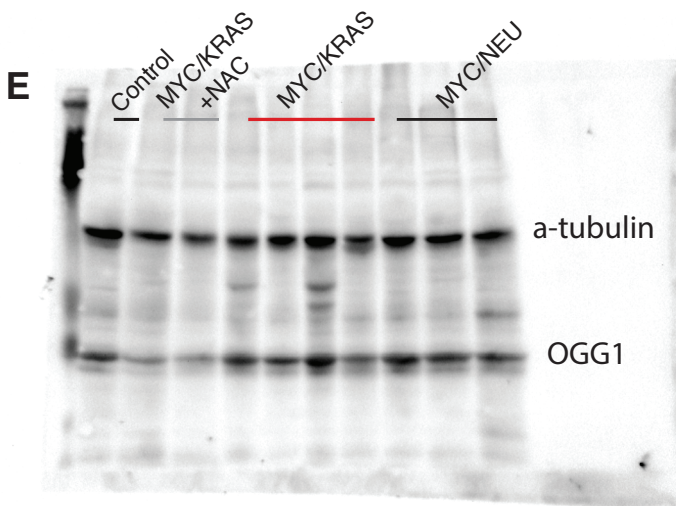
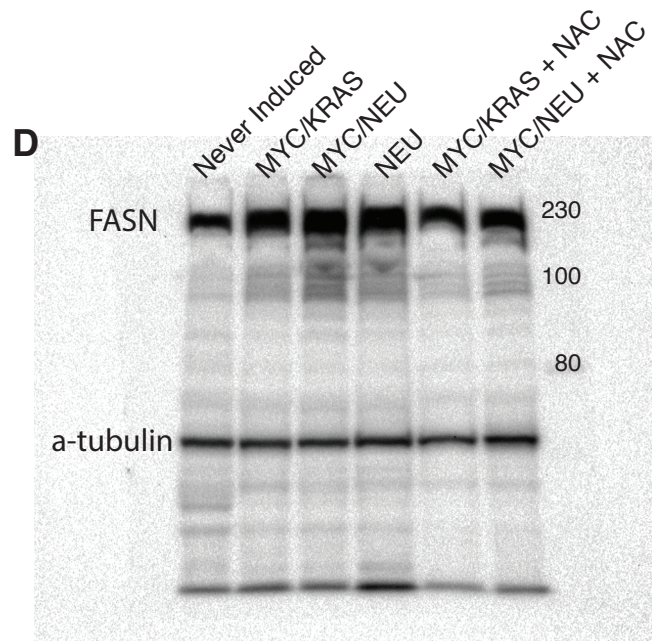
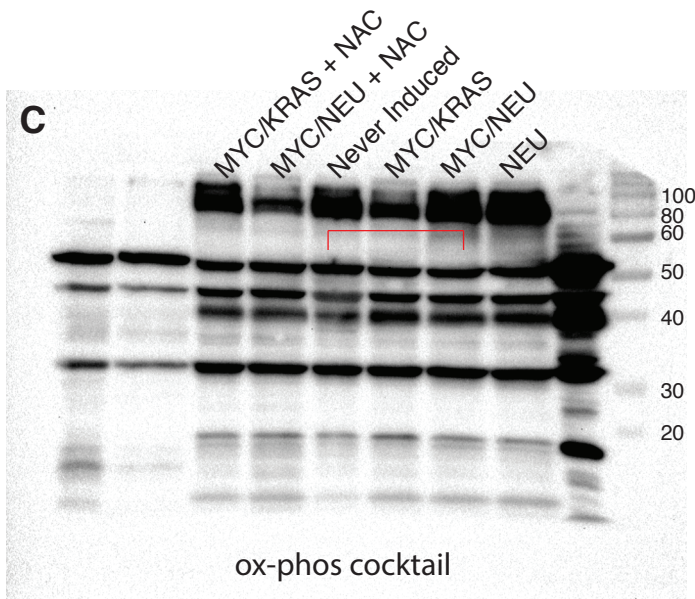
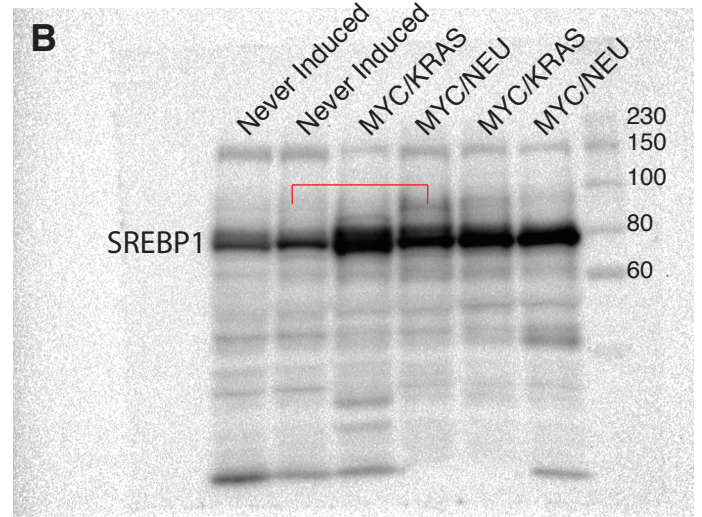
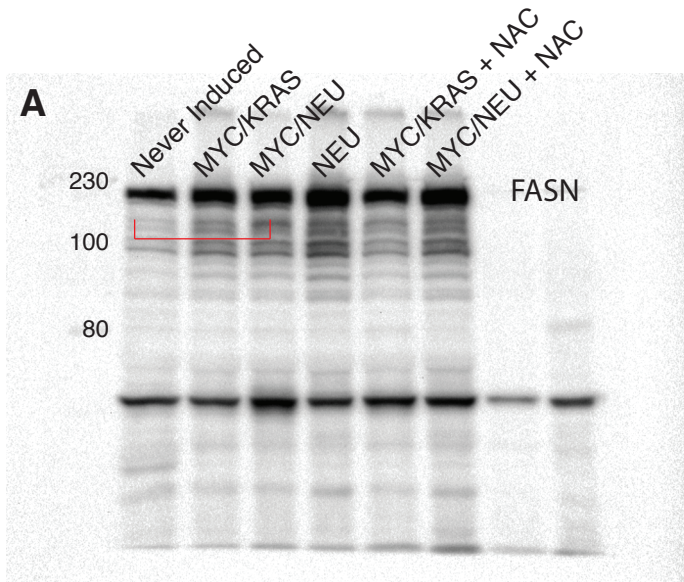
Pathways Human RNA-seq/Human GSE32072:

- Beta oxidation of decanoyl-CoA to octanoyl-CoA-CoA
- Beta oxidation of hexanoyl-CoA to butanoyl-CoA
- Beta oxidation of lauroyl-CoA to decanoyl-CoA-CoA
- Beta oxidation of octanoyl-CoA to hexanoyl-CoA
- Glutathione conjugation
- Mitochondrial Fatty Acid Beta-Oxidation
- Signaling by NOTCH1
- Synthesis of bile acids and bile salts

Metabolites Human RNA-seq/Human GSE32072:

- trans-2-cis,cis,cis-8,11,14-eicosatetraenoyl-CoA
- succinyl-CoA
- 1,2-dihydronaphthalene-1,2-diol
- 3alpha-hydroxy-5alpha-pregnan-20-one
- NADH
- 5beta-cholestan-3alpha,7alpha,12alpha-triol
- chondroitin sulfate C (GalNAc6S-GlcA), precursor 3
- methacrylyl-CoA





Un-cut Western Blots from biological replicates run on multiple gels. A. Western Blot of FASN from 8% SDS-PAGE (**Figure 3B**), B. Western blot for SREBP1 from 10% SDS-PAGE (**Figure 3B**). C. Western Blot for 5 members of the oxidative phosphorylation complex NDUFB8, CII-30kDa, CIII-Core protein 2, CIV subunit I and CV alpha subunit (**Figure 3B**), Western blot of FASN and alpha tubulin from 8% SDS-PAGE gel (**Figure 3B**), Western blot of OGG1 and alpha tubulin run on 10% SDS-PAGE gel, (**Supplementary Figure 3**)